Mitophagy in yeast is independent of mitochondrial fission and requires the stress response gene *WHI2*

Nadine Mendl[1], Angelo Occhipinti[2,3], Matthias Müller[2,3], Philipp Wild[4], Ivan Dikic[4] and Andreas S. Reichert[1,2,3,*]

[1]Adolf-Butenandt-Institut für Physiologische Chemie, Ludwig-Maximilians-Universität München, Butenandtstr. 5, 81377 München, Germany
[2]Mitochondriale Biologie, Zentrum für Molekulare Medizin, Goethe-Universität, Frankfurt am Main, Theodor-Stern-Kai 7, 60590 Frankfurt am Main, Germany
[3]Mitochondrial Biology, Frankfurt Institute for Molecular Life Sciences, Max-von-Laue-Str. 9, 60438 Frankfurt am Main, Germany
[4]Institut für Biochemie II, Fachbereich Medizin, Goethe-Universität Frankfurt am Main, Theodor-Stern-Kai 7, 60590 Frankfurt am Main, Germany
*Author for correspondence (reichert@zbc.kgu.de)

Accepted 8 December 2010
Journal of Cell Science 124, 1339-1350

doi:10.1242/jcs.076406

Summary

Dysfunctional mitochondria show a reduced capacity for fusion and, as mitochondrial fission is maintained, become spatially separated from the intact network. By that mechanism, dysfunctional mitochondria have been proposed to be targeted for selective degradation by mitophagy, thereby providing a quality control system for mitochondria. In yeast, conflicting results concerning the role of mitochondrial dynamics in mitophagy have been reported. Here, we investigate the effects on mitophagy of altering mitochondrial fission and fusion, using biochemical, as well as fluorescence-based, assays. Rapamycin-induced mitophagy was shown to depend upon the autophagy-related proteins Atg11, Atg20 and Atg24, confirming that a selective type of autophagy occurred. Both fragmentation of mitochondria and inhibition of oxidative phosphorylation were not sufficient to trigger mitophagy, and neither deletion of the fission factors Dnm1, Fis1, Mdv1 or Caf4 nor expression of dominant-negative variants of Dnm1 impaired mitophagy. The diminished mitophagy initially observed in a Δ*fis1* mutant was not due to the absence of Fis1 but rather due to a secondary mutation in *WHI2*, which encodes a factor reported to function in the general stress response and the Ras-protein kinase A (PKA) signaling pathway. We propose that, in yeast, mitochondrial fission is not a prerequisite for the selective degradation of mitochondria, and that mitophagy is linked to the general stress response and the Ras-PKA signaling pathway.

Key words: Autophagy, General stress response, Mitochondrial dynamics, Mitophagy, WHI2

Introduction

Over the past two decades, mitochondria have been recognized as a highly dynamic network constantly undergoing fusion and fission (Bereiter-Hahn and Voth, 1994; Nunnari et al., 1997). Several diseases, such as autosomal dominant optic atrophy type I (Alexander et al., 2000; Delettre et al., 2000), Charcot–Marie–Tooth neuropathy type 2A and 4A (Niemann et al., 2005; Zuchner et al., 2004) and Parkinson's disease (Banerjee et al., 2009; Exner et al., 2007; Yang et al., 2008), are associated with alterations in mitochondrial dynamics. Studies using yeast as a model organism have identified key players required for fusion and fission of mitochondria. Three proteins have been shown to be essential for mitochondrial fission, Dnm1, Fis1 and Mdv1, and these form a protein complex (Cerveny et al., 2001; Mozdy et al., 2000; Naylor et al., 2006; Otsuga et al., 1998; Sesaki and Jensen, 1999; Tieu and Nunnari, 2000). Loss of either corresponding gene results in mitochondria that display a net-like hyperfused morphology. A fourth factor, Caf4, has been reported to influence the localization of Dnm1 clusters on the mitochondrial surface, although it is not essential for fission of mitochondria (Griffin et al., 2005; Schauss et al., 2006). The mitochondrial fusion process requires Fzo1, Ugo1 and Mgm1 (Fritz et al., 2001; Hermann et al., 1998; Rapaport et al., 1998; Sesaki and Jensen, 2001; Sesaki and Jensen, 2004; Sesaki et al., 2003; Wong et al., 2000; Wong et al., 2003). Mgm1 is a large GTPase that mediates inner membrane fusion and its function has been shown to depend on mitochondria being in an intact bioenergetic state (Herlan et al., 2004; Herlan et al., 2003). In general, there is considerable knowledge on the molecular players involved in fusion and fission. However, the regulation and the functional significance of mitochondrial dynamics are still elusive.

One hypothesis is that fusion and fission dynamics act as a quality checkpoint for mitochondrial functionality (Duvezin-Caubet et al., 2006; Herlan et al., 2004; Kim et al., 2007; Lyamzaev et al., 2004; Twig et al., 2008). Our observations in yeast and mammalian cells, using several models of mitochondrial dysfunction, have shown that fusion competence is reduced when mitochondrial function is impaired (Duvezin-Caubet et al., 2006; Herlan et al., 2004). This causes dysfunctional mitochondria to become isolated from the intact network, hence providing a possible way to distinguish functional from dysfunctional mitochondria on a morphological basis; it has been hypothesized that this process could target damaged mitochondria for degradation by autophagy. Indeed, Twig and colleagues (Twig et al., 2008) have shown that, in mammalian cells, autophagy of mitochondria is impaired when fission of mitochondria is blocked and that mitochondrial depolarization precedes autophagy of mitochondria. Moreover, when autophagy is blocked, damaged mitochondria appear to accumulate (Krebiehl et al., 2010; Mortensen et al., 2010; Twig et al., 2008).

Autophagy is the process of delivering dispensable material to the lysosome or vacuole for degradation and is controlled by TOR

(target of rapamycin) signaling (Carrera, 2004; Noda and Ohsumi, 1998; Yang and Klionsky, 2009). It comprises several pathways that differ in the selected cargo, as well as in the delivery pathway to the vacuole. Macroautophagy is characterized by degradation of cytosol in bulk and is therefore considered nonselective. Selective types of autophagy include the cytoplasm-to-vacuole targeting (Cvt) pathway, which delivers specific proteins to their final destination in the vacuole, as well as mitophagy and pexophagy, which, for example, remove superfluous organelles upon a shift of carbon source. Studies on the molecular mechanism of autophagy in yeast have identified several proteins involved in the process, termed the autophagy-related (Atg) proteins (Huang and Klionsky, 2007; Klionsky et al., 2003). Most of these proteins are required for all autophagy pathways; for example, Atg1 is required for autophagy induction and Atg8 for the formation of the cargo transport vesicle (the autophagosome). Selective types of autophagy are further characterized by recognition and targeting of the cargo, which is mediated by Atg11, Atg20 and Atg24 (Nice et al., 2002; Yorimitsu and Klionsky, 2005).

Less is known about the factors that influence the selective degradation of mitochondria, known as mitophagy. Recent reports confirm that mitochondria can be selectively targeted for autophagy (Kanki and Klionsky, 2008; Kim et al., 2007). In mammalian systems, PINK1 and PARKIN have been shown to be involved in targeting depolarized mitochondria to autophagosomes (Geisler et al., 2010; Narendra et al., 2010). Furthermore, NIX (BNIP3L) has been identified as an essential requirement for elimination of mitochondria during erythrocyte differentiation (Sandoval et al., 2008; Schweers et al., 2007) and has been shown recently to act as a selective receptor for mitophagy, interacting physically with LC3A (MAP1LC3A) and all GABARAP proteins (GABARAP, GABARAPL1, GABARAPL2) (Novak et al., 2010). In yeast, mitophagy has been suggested to depend on Uth1 (Kissova et al., 2004), Aup1 (Tal et al., 2007) and proteins required for selective forms of autophagy, namely Atg11, Atg20 and Atg24 (Kanki and Klionsky, 2008). Recently, Atg32 has been identified in two independent screens for yeast strains deficient in mitophagy (Kanki et al., 2009b; Okamoto et al., 2009). Furthermore, it has been shown that this factor is located at the mitochondrial outer membrane and thus it has been proposed to act as a receptor for targeting mitochondria to the autophagosomal membrane. In addition, Atg33 has been identified in one of the screens as being required for mitophagy (Kanki et al., 2009a). So far, mitophagy in yeast has been observed upon mitochondrial dysfunction (Nowikovsky et al., 2007; Priault et al., 2005), in stationary phase (Okamoto et al., 2009; Tal et al., 2007), and upon nitrogen starvation (Kanki and Klionsky, 2008; Kissova et al., 2007) and rapamycin treatment (Kissova et al., 2004). The latter two conditions are known to inhibit TOR signaling, which also leads to a general induction of autophagy (Carrera, 2004; Noda and Ohsumi, 1998).

The molecular mechanisms and the regulation of mitophagy remain largely unclear. Here, we focus on deciphering the role of mitochondrial dynamics in mitophagy in yeast. In particular, the role of mitochondrial fission is debated; whereas in mammalian cells fission has been shown to be required for mitophagy (Twig et al., 2008), two screens performed in yeast revealed apparently conflicting results in this regard. One study reported reduced induction of mitophagy upon nitrogen starvation in a *dnm1* deletion strain, whereas deletion strains for the other mitochondrial fission factors, Mdv1, Fis1 and Caf4, did not show such a defect (Kanki et al., 2009a). A different study was unable to show that Dnm1, Mdv1, Caf4 or Fis1 has any effect on mitophagy (Okamoto et al., 2009). By contrast, induction of mitophagy, as observed by loss of Mdm38 function, has been proposed to depend upon Dnm1 (Nowikovsky et al., 2007). It is thus not resolved whether mitochondrial fission is required for mitophagy in yeast.

Our present data show no direct correlation between mitochondrial morphology and mitophagy. Fragmentation of mitochondria was not sufficient to induce mitophagy. In strains defective in mitochondrial fission, induction of mitophagy was as efficient as in wild-type strains. Reduced mitophagy activities were initially observed in a *fis1* deletion strain (*Δfis1*) but not in any other fission mutant or upon expression of various dominant-negative variants of Dnm1. However, we found that the effect observed in *Δfis1* was due to a secondary mutation in the locus of the stress response gene *WHI2* (*Whiskey 2*). This genetic suppression had been reported previously to arise in Δ*fis1* and is responsible for an overgrowth phenotype in stationary phase (Cheng et al., 2008). Whi2 was suggested to regulate cell cycle control, as Δ*whi2* cells fail to enter G1 and arrest randomly within the cell cycle in stationary phase (Radcliffe et al., 1997; Sudbery et al., 1980). Moreover, Δ*whi2* mutants fail to accumulate storage glycogen and are sensitive to environmental stresses, such as heat shock. A later study provided the first biochemical evidence for its function in the regulation of Msn2 phosphorylation, thereby implicating a function for Whi2 in the general stress response (Kaida et al., 2002). Recently, it has been suggested that Whi2 influences the subcellular localization of Ras2, linking it to the Ras-protein kinase A (PKA) signaling pathway (Leadsham et al., 2009). Our present data demonstrate that Whi2 is required for an efficient induction of mitophagy, which could point to a link between TOR, Ras-PKA signaling, autophagy and the general stress response pathway. In summary, we suggest that fragmentation is neither the sole signal of mitochondrial dysfunction nor a prerequisite for mitochondria to be targeted for degradation in yeast.

Results

Mitophagy induced by rapamycin is a selective form of autophagy

In order to determine the extent of mitophagy, as well as autophagy, in a quantitative manner, we employed the modified alkaline phosphatase (ALP) assay described previously (Campbell and Thorsness, 1998; Noda et al., 1995). In a strain lacking the endogenous alkaline phosphatase Pho8, we expressed an inactive proenzyme of Pho8 that was targeted to either the mitochondrial matrix (mtPho8) or the cytosol (cytPho8). We confirmed the correct localization of both mtPho8 and cytPho8 by cell fractionation and proteinase K treatment (supplementary material Fig. S1B,C) and that neither deletion of *PHO8* nor expression of these constructs impaired the growth of yeast cells (supplementary material Fig. S1A). It is known that proenzyme Pho8 is activated upon proteolytic processing by proteinase A (*PEP4*) within the vacuole. We found that the specific activities of mtPho8 and cytPho8 increased significantly when the respective strains were grown under nitrogen starvation or after addition of rapamycin (supplementary material Fig. S2A,B). ALP activities in the mock-treated cells and in cells lacking proteinase A (Δ*pep4*) remained at background levels, confirming that mtPho8 and cytPho8 are exclusively activated in the vacuole and that background activities of other proteases and phosphatases do not impair the assay. We conclude that the increase

in mtPho8 and cytPho8 activity reflects induction of mitophagy and autophagy, respectively.

First, we asked whether induction of mitophagy by rapamycin is a selective type of autophagy or whether it instead represents a random sequestration of mitochondria upon induction of bulk autophagy. Therefore, we investigated the induction of mitophagy and autophagy in mutants known to be deficient in selective types of autophagy, such as mitophagy, pexophagy and the Cvt pathway. Deletion of *atg11* completely prevented induction of mitophagy by rapamycin but did not grossly impair bulk autophagy (Fig. 1A,B). Furthermore, mitophagy but not autophagy was reduced to ~40% in the *atg20* and *atg24* deletion strains (Fig. 1A,B), which is consistent with the known partial effect on mitophagy of these mutants (Kanki and Klionsky, 2008). Neither mitophagy nor

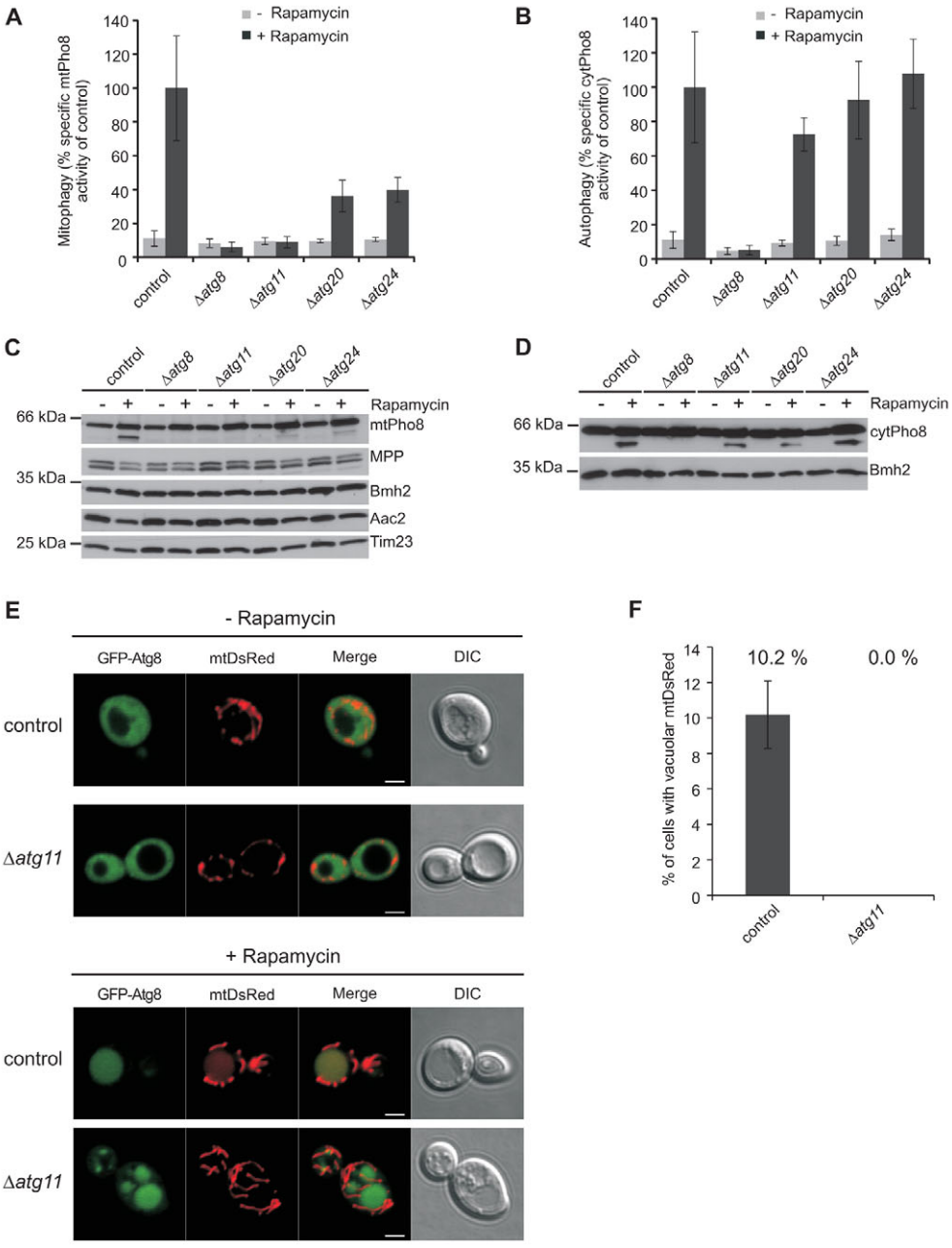

Fig. 1. Rapamycin specifically induces mitophagy. (**A**–**D**) Strains deleted for the indicated gene, and for endogenous *pho8*, expressing mtPho8 (A,C) or cytPho8 (B,D) were analyzed during exponential growth (– rapamycin) or after rapamycin treatment for 24 hours and compared with control strains. Control represents the Δ*pho8* strain expressing mtPho8 (A,C) or cytPho8 (B,D). Mitophagy (A) and autophagy (B) were quantified by the ALP assay as described in the Materials and Methods. Specific activities of mtPho8 and cytPho8 are given as means ± s.d. ($n \geq 4$) normalized to the mean of the treated control. Levels of mitochondrial markers (Tim23, Aac2 and MPP) and proteolytic activation of mtPho8 (C) and cytPho8 (D) were determined by SDS-PAGE and western blotting. Bmh2 served as the loading control. (**E**) Δ*atg11* and wild-type (control) strains expressing mtDsRed and GFP–Atg8 were analyzed for mitophagy and autophagy by confocal fluorescence microscopy after treatment with DMSO (– rapamycin) or rapamycin for 7.5 hours. Single confocal planes are shown. Scale bars: 2 µm. (**F**) Accumulation of mtDsRed in the vacuole was quantified in cells treated with rapamycin as in panel E. Results are means ± s.d. (n=3).

autophagy was induced in a strain lacking the essential autophagy component Atg8 (Fig. 1A,B), further confirming the specificity of the ALP assay. To corroborate these results, we analyzed cell lysates of the aforementioned strains by SDS-PAGE and western blotting (Fig. 1C,D). The extent of the processing of Pho8 in the individual strains was consistent with the measured alkaline phosphatase activities, confirming that rapamycin-induced mitophagy depends upon Atg11, Atg20 and Atg24. In addition, we monitored the total levels of Tim23, a subunit of the mitochondrial TIM23 translocase, Aac2, the major ADP/ATP carrier of the inner membrane, and MPP, the mitochondrial processing peptidase. The levels of these markers decreased upon addition of rapamycin in the control strain but only marginally decreased in the strains deleted for either *atg8* or *atg11*, demonstrating further that the degradation of mitochondria occurs in a selective manner. In the Δ*atg20* and Δ*atg24* strains, the levels of Tim23, Aac2 and MPP were diminished, to some extent, upon addition of rapamycin, which is consistent with the partial induction of mitophagy observed by the ALP assay. In general, we noted that monitoring mitophagy by western blotting of mitochondrial markers gave considerably more variable results. We attribute this to varying activities of vacuolar and mitochondrial proteases, either pre- or post-lysis, which are likely to affect the extent of degradation of individual marker proteins in an unequal and not entirely reproducible manner. By contrast, the ALP assay is very reproducible and specifically monitors the activation of the inactive proenzyme Pho8 within the vacuole without showing any Pep4-independent activation (e.g. by cytosolic or intramitochondrial proteolysis).

In addition, to further corroborate the biochemical results, we performed a visual assay for mitophagy. Cells expressing GFP–Atg8 and mtDsRed were analyzed by confocal fluorescence microscopy after rapamycin treatment. In mock-treated cells, GFP–Atg8 was evenly distributed in the cytosol and mtDsRed labeled a typical mitochondrial network. Upon treatment with rapamycin, accumulation of GFP in the vacuole was observed in nearly all cells, indicating that GFP–Atg8 was efficiently shuttled to the vacuole and that there was autophagy (Fig. 1E). Upon rapamycin treatment, the mitochondrial mtDsRed signal was unambiguously detectable in the vacuole in ~10% of the control cells but in none of the cells lacking Atg11 (Fig. 1E,F). Thus, according to this visual assay, as well as the biochemical assays, induction of mitophagy by rapamycin depended upon Atg11. In summary, we conclude that, upon rapamycin treatment, mitochondria are degraded through a selective form of autophagy and that the modified ALP assay used provides a reliable, quantitative and sensitive way of monitoring mitophagy and autophagy in yeast.

Fragmentation of mitochondria is not sufficient to trigger mitophagy

In order to assess whether fragmentation of mitochondria is sufficient to trigger mitophagy, we used the temperature-sensitive *mgm1-5* strain, which shows defective inner membrane fusion at the non-permissive temperature of 37°C (Wong et al., 2000). The mitochondrial morphology of the *mgm1-5* strain and a corresponding wild-type strain, both expressing mtPho8 and mtDsRed, was determined at 24°C and 37°C. At the non-permissive

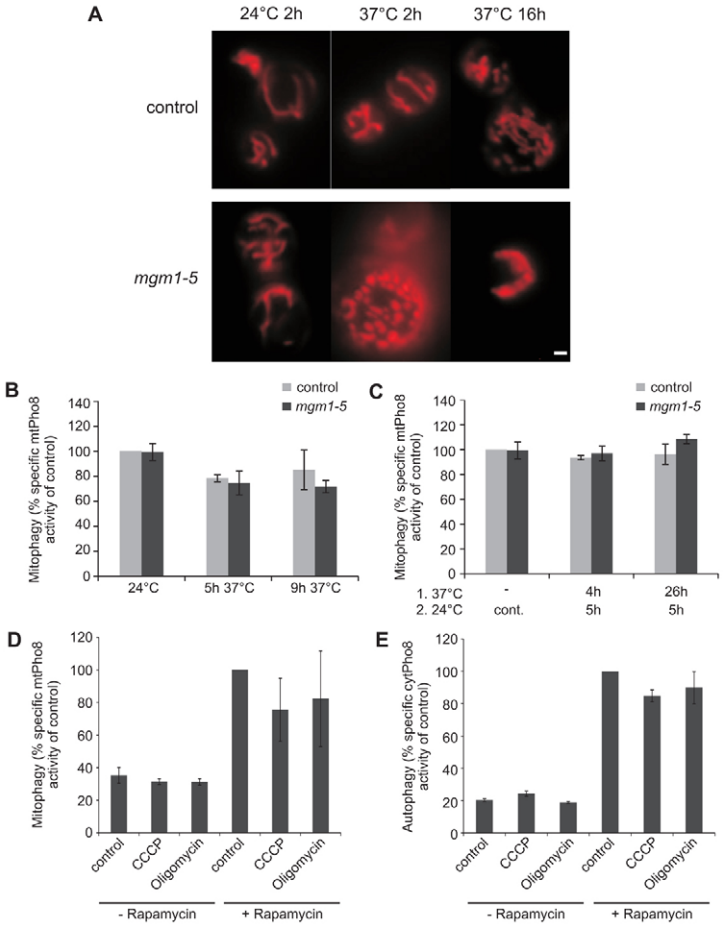

Fig. 2. Mitochondrial fragmentation does not trigger mitophagy. (**A**) Wild-type (control) or *mgm1-5* mutant cells expressing mtDsRed were incubated at 24°C or 37°C in SG for the indicated times and their mitochondrial morphology was examined by fluorescence microscopy. Scale bar: 1 µm. (**B**) Wild-type (control) and *mgm1-5* strains, deleted for endogenous *pho8* and expressing mtPho8, were incubated at 24°C or 37°C for the indicated time and mitophagy was determined by measuring the mtPho8 activity (ALP assay). Specific mtPho8 activities are normalized to that in the control at 24°C and are given as means ± s.d. (*n*=3). (**C**) Strains, as described in B, were incubated at 24°C or 37°C for the indicated times, followed by incubation at 24°C for 5 hours, to allow the mitochondrial morphology to recover, and were analyzed with the ALP assay. Specific mtPho8 activities are normalized to that of the control at 24°C and are given as means ± s.d. (*n*=3). (**D**,**E**) Wild-type cells, deleted for endogenous *pho8* and expressing mtPho8 (D) or cytPho8 (E), were treated with 10 µM CCCP or oligomycin in the presence or absence of rapamycin for 5 hours. Mitophagy (D) and autophagy (E) were quantified with the ALP assay. Specific activities of mtPho8 and cytPho8 are normalized to that in untreated cells incubated with rapamycin (control + rapamycin) and are given as means ± s.d. (*n*=3).

temperature, the *mgm1-5* strain showed a complete fragmentation of mitochondria after 2 hours of incubation and an aggregation of mitochondria after 16 hours of incubation (Fig. 2A), consistent with published data for this strain (Wong et al., 2000). The wild-type control maintained the typical tubular network of mitochondria at both temperatures. Next, we analyzed mitophagy by the ALP assay at different time points of incubation at the non-permissive temperature. ALP activity remained at background levels for both strains after 5 or 9 hours of incubation, indicating that mitophagy was not induced by fragmentation of mitochondria (Fig. 2B). Next, we tested whether temporary fragmentation of mitochondria for 5 or 26 hours at the non-permissive temperature, followed by a shift back to the permissive temperature for 5 hours, would trigger mitophagy. However, shifting back to the permissive temperature also did not result in increased ALP activity (Fig. 2C). We conclude that fragmentation of mitochondria alone is not sufficient to trigger mitophagy. To exclude the possibility that a shift to 37°C, or impairing Mgm1 function itself, blocks mitophagy, we confirmed that rapamycin was still able to induce mitophagy efficiently at the permissive and the non-permissive temperature in both strains (data not shown). Furthermore, we observed that rapamycin treatment alone did not result in mitochondrial fragmentation, showing that fragmentation does not precede mitophagy in yeast (Fig. 1E; supplementary material Fig. S3). Rapamycin did not have a general impact upon the ability of mitochondria to generate an electrochemical gradient across the inner membrane, as mitochondria were still efficiently labeled by the membrane-potential-sensitive dye Rhodamine B hexyl ester (supplementary material Fig. S3). However, we cannot exclude a minor effect of rapamycin on the mitochondrial membrane potential, as there was a slight reduction in signal intensity. Nevertheless, fusion and fission of mitochondria proceeded in a normal manner after rapamycin treatment, in accordance with the overall wild-type-like mitochondrial morphology (Fig. 1E; supplementary material Fig. S3) and time-lapse fluorescence microscopy (data not shown). Thus, rapamycin itself does not appear to alter mitochondrial dynamics or cause major mitochondrial dysfunction.

Drug-induced mitochondrial dysfunction is not sufficient to induce mitophagy in yeast

It has been reported, for mammalian cells, that mitophagy and autophagy are induced by drugs that impair mitochondrial oxidative phosphorylation (Chen et al., 2007; Ding et al., 2010; Novak et al., 2010). To test whether this is also the case in yeast, we treated cells for 5 hours with carbonyl cyanide *m*-chlorophenylhydrazone (CCCP) to dissipate the mitochondrial membrane potential. We did not observe any induction of mitophagy or autophagy (Fig. 2D,E). Addition of CCCP efficiently dissipated the membrane potential, as virtually no mitochondrial labeling, but instead only weak cytosolic labeling, was observed using the membrane-potential-sensitive dye Rhodamine B hexyl ester (supplementary material Fig. S3). Furthermore, this treatment resulted in a fragmented mitochondrial morphology, consistent with the fact that mitochondrial fusion is inhibited in the absence of a membrane potential (Legros et al., 2002; Meeusen et al., 2004). In addition, a longer incubation (up to 24 hours) with CCCP did not lead to any induction of mitophagy or autophagy (data not shown). Thus, even CCCP-induced fragmentation of mitochondria is not sufficient to induce mitophagy. Induction of mitophagy or autophagy was also not observed when the F_1F_o-ATPase inhibitor oligomycin was used (Fig. 2D,E). Moreover, neither CCCP nor oligomycin treatment impaired rapamycin-induced mitophagy or autophagy, demonstrating that the ALP assay was not inhibited per se. In addition, these drugs did not exert a stimulatory effect on rapamycin-induced mitophagy. Taken together, these results show that induction of mitophagy is not triggered by mitochondrial fragmentation or inhibition of oxidative phosphorylation and apparently is mechanistically distinct between mammalian and yeast cells.

Expression of a dominant-negative variant of Dnm1 does not impair mitophagy

Next, we asked whether blocking mitochondrial fission inhibits mitophagy in yeast. We expressed Dnm1 variants with a dominant-negative effect on mitochondrial fission (Otsuga et al., 1998), and quantified the induction of mitophagy and autophagy upon rapamycin treatment. Expression of $Dnm1^{K41A}$ and $Dnm1^{S42N}$ resulted in a fishnet-like hyperfused mitochondrial morphology, confirming that these variants indeed exerted a dominant-negative effect (data not shown). Upon rapamycin treatment, ALP activities for mtPho8 and cytPho8 increased to a similar extent in the strains expressing the dominant-negative variants of Dnm1 to that in the control strains (Fig. 3A,B), indicating that neither mitophagy nor autophagy are affected when mitochondrial fission is impaired. We further confirmed that induction of mitophagy still depended upon Atg11, excluding the possibility that a non-selective type of mitophagy was induced upon expression of wild-type or dominant-negative variants of Dnm1 (supplementary material Fig. S4A). Western blotting revealed that processing of the proenzymes of

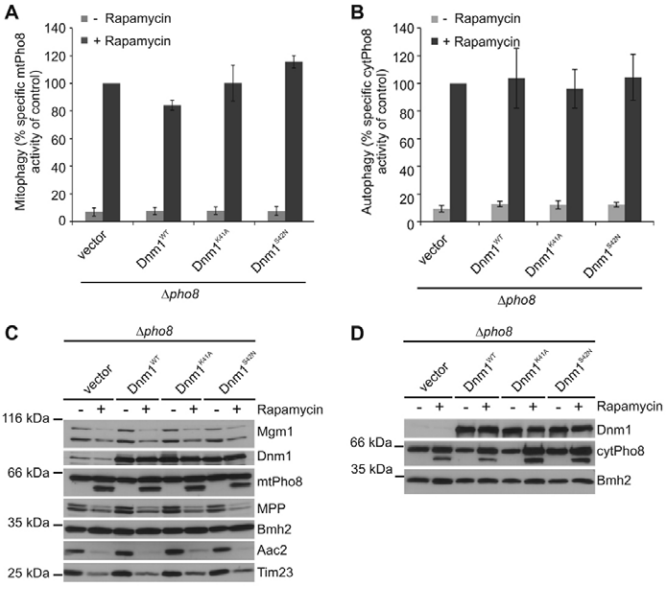

Fig. 3. Expression of dominant-negative Dnm1 does not inhibit mitophagy. (**A**–**D**) Strains expressing wild-type (WT) or the indicated mutant Dnm1, and mtPho8 (A) or cytPho8 (B), were analyzed during exponential growth (– rapamycin) and after rapamycin treatment for 24 hours. Mitophagy (A) and autophagy (B) were quantified with the ALP assay as described in the Materials and Methods. Specific activities of mtPho8 and cytPho8 are given as means ± s.d. (n=3), normalized to the mean of the rapamycin-treated strain containing empty vector. Levels of the mitochondrial markers (Tim23, Aac2, MPP and Mgm1) and Dnm1, and proteolytic activation of mtPho8 (C) and cytPho8 (D), were determined by SDS-PAGE and western blotting. Bmh2 served as the loading control.

mtPho8 or cytPho8 was not impaired by expression of the dominant-negative variants of Dnm1, consistent with the ALP activities determined above (Fig. 3C,D). In addition, rapamycin-induced degradation of the mitochondrial markers Tim23, Aac2 and MPP was not impaired in the presence of these Dnm1 variants, thereby confirming that inhibiting mitochondrial fission does not block mitophagy (Fig. 3C). The level of the fusion factor Mgm1 was affected in a similar way upon rapamycin addition but did not show any altered expression under conditions without rapamycin (Fig. 3C). In summary, these data suggest that mitophagy in yeast is independent of mitochondrial fission.

Fission of mitochondria is not a prerequisite for mitophagy in yeast

It cannot be ruled out that, upon expression of dominant-negative variants of Dnm1, a residual mitochondrial fission activity, sufficient for mitophagy, remained. To address this in more detail, we analyzed induction of mitophagy in strains lacking one of the fission factors Dnm1, Mdv1, Caf4 or Fis1. Consistent with the mitochondrial morphology reported earlier for these strains (Cerveny et al., 2001; Griffin et al., 2005; Mozdy et al., 2000; Naylor et al., 2006; Otsuga et al., 1998; Schauss et al., 2006; Sesaki and Jensen, 1999; Tieu and Nunnari, 2000), we observed a fishnet-like hyperfused mitochondrial morphology for the Δ*dnm1*, the Δ*mdv1* and the Δ*fis1* strains, and a more wild-type-like tubular morphology for the Δ*caf4* strain (Fig. 4E; supplementary material Fig. S4B; data not shown). We did not observe an alteration of mitochondrial appearance upon addition of rapamycin in any of these strains (Fig. 4E; supplementary material Fig. S4B; data not shown). The correct localization of mtPho8 in these mutant strains was confirmed by cellular subfractionation and western blotting (supplementary material Fig. S1D). Consistent with results obtained

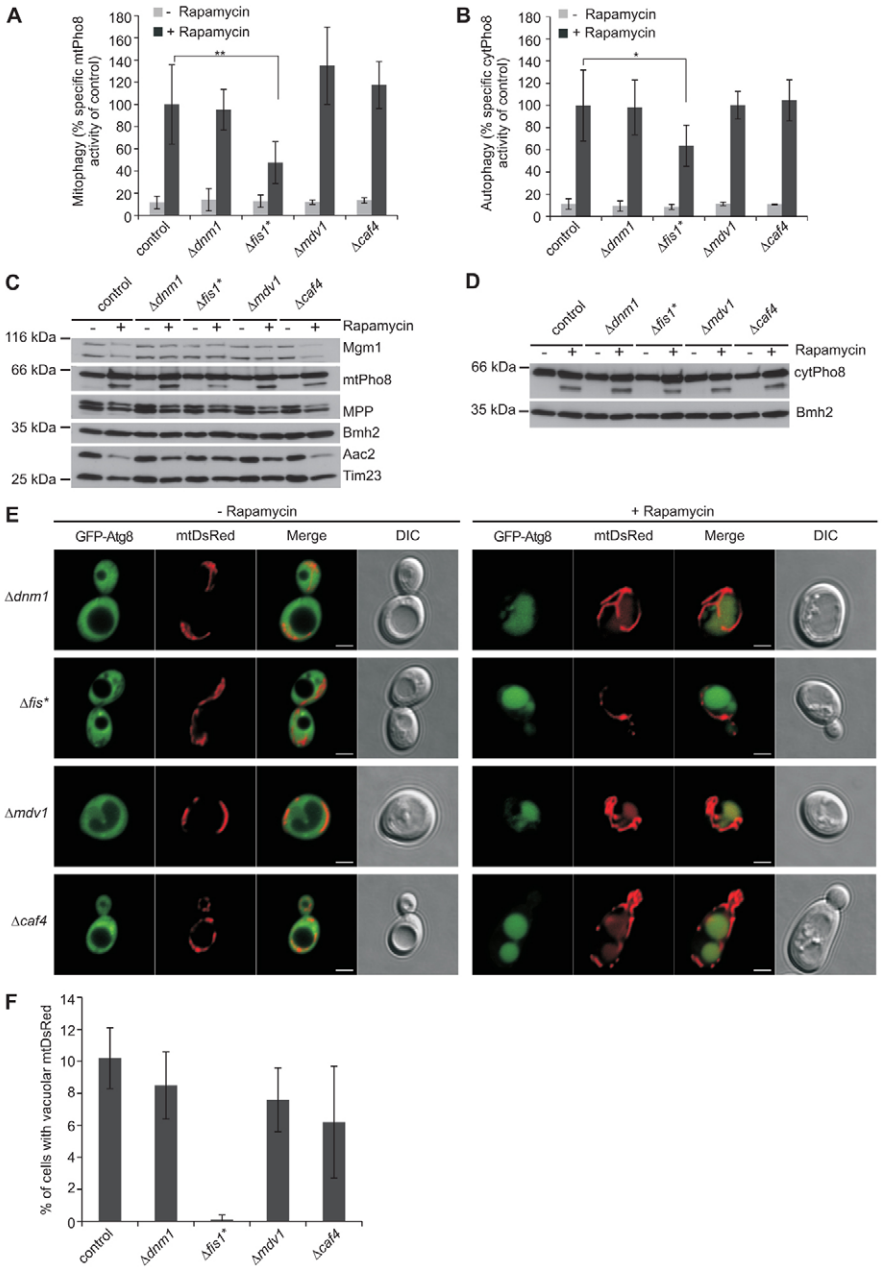

Fig. 4. Mitophagy and autophagy are impaired in Δ*fis1 but not in other fission mutants.**
(**A**–**D**) Strains deleted for the indicated gene and for endogenous *pho8*, expressing mtPho8 (A,C) or cytPho8 (B,D), were analyzed during exponential growth (– rapamycin) or after rapamycin treatment for 24 hours and compared with the control strain. Control represents the wild-type strain deleted for *pho8* and expressing mtPho8 (A,C) or cytPho8 (B,D). Δ*fis1** refers to the EUROSCARF strain containing a suppressor mutation (see Fig. 5A). Mitophagy (A) and autophagy (B) were quantified with the ALP assay as described in the Materials and Methods. Specific activities of mtPho8 and cytPho8 are given as means ± s.d. ($n \geq 4$) normalized to the mean of the rapamycin-treated control. *$P<0.005$; **$P<0.001$. The levels of the mitochondrial markers (Tim23, Aac2, Mgm1 and MPP) and the proteolytic activation of mtPho8 (C) or cytPho8 (D) were determined by SDS-PAGE and western blotting. Bmh2 served as the loading control. (**E**) The indicated strains expressing mtDsRed and GFP–Atg8 were analyzed for mitophagy and autophagy by confocal fluorescence microscopy after treatment with DMSO (– rapamycin) or rapamycin for 7.5 hours. Single confocal planes are shown. Scale bars: 2 µm. (**F**) Accumulation of mtDsRed in the vacuole was quantified in cells treated with rapamycin as in panel E. Results are means ± s.d (n=3).

using dominant-negative Dnm1 variants, the Δ*dnm1* strain showed a normal increase in mtPho8 or cytPho8 activity upon rapamycin treatment, confirming that Dnm1-dependent fission is not required for mitophagy or autophagy (Fig. 4A,B). The same result was obtained for the Δ*mdv1* and Δ*caf4* strains, further corroborating that fission is not a prerequisite for mitophagy or autophagy. In line with these results, we did not observe a physical interaction of these fission components with Atg8 using a yeast two-hybrid approach (data not shown). We also noted that CCCP and oligomycin did not induce mitophagy or autophagy, nor did they lead to an inhibition of rapamycin-induced mitophagy or autophagy in the Δ*dnm1* strain (supplementary material Fig. S4C,D). Thus, under hyperfused conditions, the ability of mitochondria to generate ATP or a membrane potential is also not required for these processes. However, the Δ*fis1* strain showed ~50% less induction of mitophagy and ~30% less induction of autophagy, when treated with rapamycin (Fig. 4A,B). These results were corroborated by western blotting (Fig. 4C,D) and the visual assay for mitophagy (Fig. 4E,F). Notably, we often observed a more intense GFP–Atg8 signal intensity in the Δ*fis1* strain compared with that in control cells (data not shown); this could be due to a decreased turnover or an increased expression of GFP–Atg8 in this strain.

We next undertook experiments to determine the cause of the apparent discrepancy regarding the effect on mitophagy in the different fission mutants. It had been reported that a secondary mutation in the *WHI2* locus was present in a Δ*fis1* strain obtained from the EUROSCARF clone collection (Cheng et al., 2008). As it will become evident below, the Δ*fis1* strain from EUROSCARF we used also contained this secondary mutation. We thus refer to this strain as Δ*fis1**. In summary, although mitophagy can occur independently from fission, it seems to be reduced in the Δ*fis1** deletion strain.

WHI2 is required for induction of mitophagy

To address whether Fis1 plays a mechanistic role, possibly distinct from fission, in mitophagy or whether the observed impairment in mitophagy was due to a *whi2* mutation, we checked the Δ*fis1** strain for a potential *whi2* mutation. Sequencing of a PCR product amplified from the *WHI2* locus identified the same mutation (T206G) in Δ*fis1** as reported by Cheng and colleagues (Cheng et al., 2008); this mutation introduces a premature stop codon after 68 amino acids (Fig. 5A). As wild-type Whi2 consists of 486 amino acids, it is probable that the early stop codon results in a complete loss of function. Consequently, we analyzed Whi2 for its role in mitophagy and autophagy. Indeed, induction of mitophagy was significantly reduced in the Δ*whi2* strain (Fig. 5B), resembling the effect in the Δ*fis1** strain. Induction of autophagy was decreased by ~10% in the Δ*whi2* strain, although this decrease was not statistically significant (Fig. 5C). The visual mitophagy assay using confocal fluorescence microscopy revealed that mtDsRed accumulation in the vacuole was markedly reduced in Δ*whi2* compared with that in the control strain, confirming the result

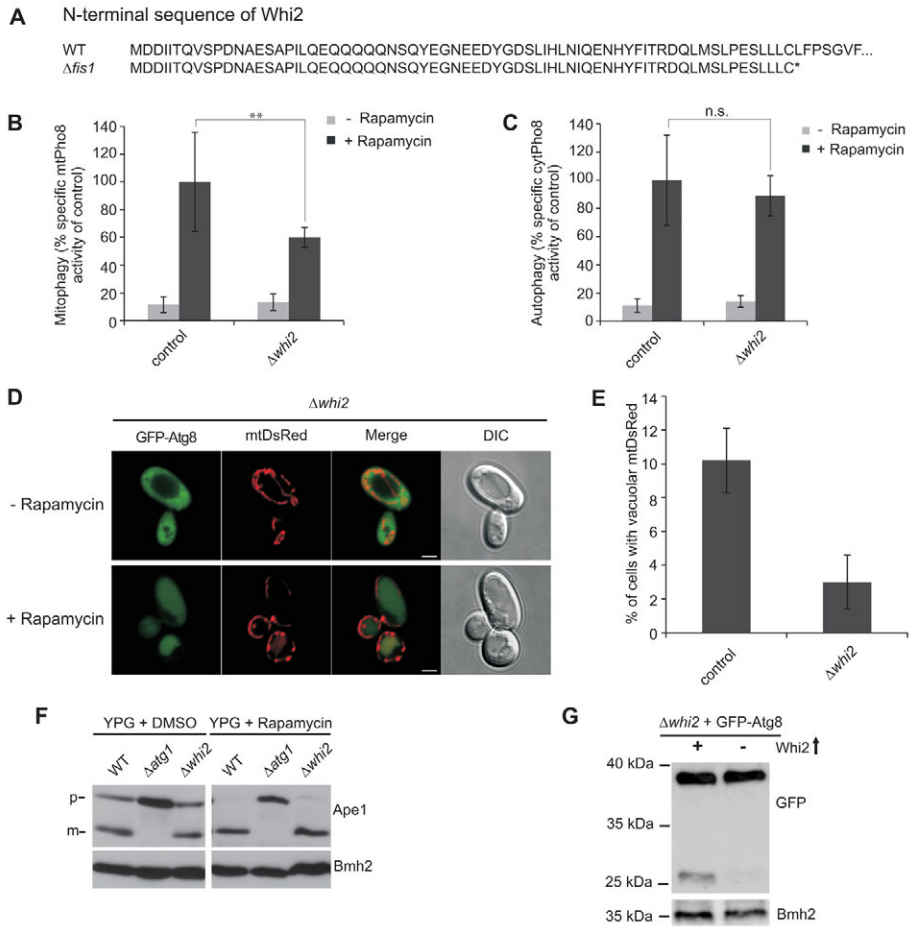

Fig. 5. Mitophagy is impaired in Δ*whi2*. (**A**) The Whi2 protein sequence was obtained by sequencing the DNA of the *WHI2* locus from Δ*fis1**, supplied by EUROSCARF, and was compared with the Whi2 wild-type (WT) sequence. The point mutation observed in Δfis1* results in a premature stop codon in *WHI2* after amino acid residue 68. (**B**,**C**) Δ*whi2* or the control strain (Δ*pho8*), expressing mtPho8 or cytPho8, were analyzed during exponential growth (– rapamycin) or after rapamycin treatment for 24 hours. Mitophagy (B) and autophagy (C) were quantified with the ALP assay as described in the Materials and Methods. Specific activities of mtPho8 and cytPho8 are given as means ± s.d. ($n \geq 5$) normalized to the mean of the rapamycin-treated control. $^{**}P<0.001$. (**D**) Δ*whi2* cells expressing mtDsRed and GFP–Atg8 were analyzed for mitophagy and autophagy by confocal fluorescence microscopy after treatment with DMSO (– rapamycin) or rapamycin for 7.5 hours. Single confocal planes are shown. Scale bars: 2 µm. (**E**) Accumulation of mtDsRed in the vacuole was quantified in cells treated with rapamycin as in D. Results are means ± s.d. (n=3). (**F**) Wild-type or strains deleted for indicated genes were grown in yeast extract peptone glycerol and treated with DMSO or rapamycin for 5 hours. Processing of Ape1 from the precursor (p) to the mature (m) form was analyzed by SDS-PAGE and western blotting. Bmh2 served as the loading control. (**G**) Δ*whi2* cells constitutively expressing GFP–Atg8 and overexpressing (+) or not overexpressing (–) Whi2–His_9 (Whi2↑) were analyzed during exponential growth in SG medium. Processing of GFP–Atg8 was determined by SDS-PAGE and western blotting. Bmh2 served as the loading control.

obtained by the ALP assay (Fig. 5D,E). These data suggest that the mitophagy phenotype in the Δ*fis1** could indeed result from the loss of function of Whi2. Given these observations, we asked whether loss of Whi2 was specific to mitophagy and decided to test whether it could also affect the Cvt pathway. We found that Ape1 processing, and the increased Ape1 processing induced by rapamycin, was dependent on Atg1, as reported previously (Kim et al., 2001; Kim et al., 2002), but was not dependent on Whi2 (Fig. 5F). We conclude that Whi2 plays no general role in selective types of autophagy. In addition, we noted that overexpression of Whi2 in a strain expressing GFP–Atg8 led to an increased processing of the GFP moiety compared with that in the control strain lacking Whi2 (Fig. 5G). This suggests that Whi2 is functionally linked to Atg8 and appears to positively modulate autophagic flux in yeast cells. Taken together, we propose that Whi2 is a factor predominantly affecting mitophagy and, to a lesser extent, autophagy.

Mitophagy is impaired in *Δfis1** owing to a secondary loss-of-function mutation in *WHI2*

To address further the role of Fis1 and Whi2 in mitophagy, we expressed Whi2 and Fis1 from a low-copy-number plasmid under their respective endogenous promoters in the Δ*fis1** and the Δ*whi2* strains. The ALP assay showed a recovery of mitophagy upon rapamycin treatment only when Whi2 was expressed but not when Fis1 was expressed (Fig. 6A). In addition, efficient induction of autophagy was only observed when wild-type Whi2 was reintroduced (Fig. 6B). These results were further confirmed by western blotting, as mtPho8 processing was more pronounced when Whi2 was expressed compared with that in the situations when functional Whi2 was lacking (Fig. 6C,D). In addition, rapamycin-induced reductions in the levels of the mitochondrial marker proteins Tim23, Aac2 and MPP were prominent when Whi2 was expressed, but were less pronounced in the absence of functional Whi2 (Fig. 6C,D). However, some Whi2-independent degradation of mitochondrial markers was detectable; we attribute this to the fact that mitophagy is not fully blocked in the absence of Whi2 and that, according to our own experience, western blotting is of limited reliability to monitor mitophagy. The efficient recovery of mitophagy upon expression of Whi2, but not Fis1, was also observed using the visual mitophagy assay (Fig. 6E). Using this assay, it appeared that the expression of Fis1 slightly promoted mitophagy. However, this minor increase was not significant and can be attributed to the rather high variation observed in the strains using this assay. Finally, we also generated a Δ*fis1* strain in a w303 background and confirmed by DNA sequencing that no suppressor mutation in the *WHI2* gene was present. This strain did not show any impairment in the induction of mitophagy or autophagy by rapamycin (supplementary material Fig. S5A–C). Overall, several lines of evidence demonstrate that Whi2, but not Fis1, is required to fully induce mitophagy and autophagy after rapamycin treatment.

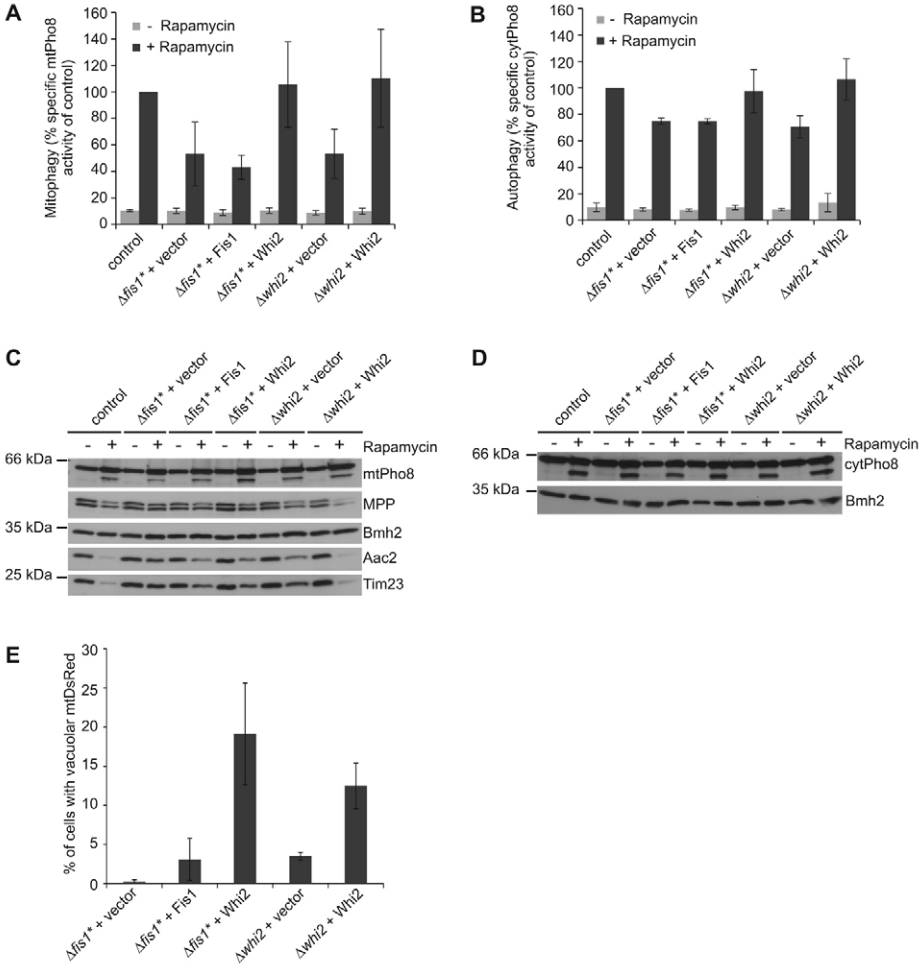

Fig. 6. Expression of Whi2 but not Fis1 complements the mitophagy and autophagy phenotype in Δ*fis1.** (**A**–**D**) The indicated strains deleted for endogenous *pho8*, expressing mtPho8 (A,C) or cytPho8 (B,D), and containing empty vector, Fis1 or Whi2, were analyzed during exponential growth (– rapamycin) and after rapamycin treatment for 24 hours. Control represents the wild-type strain deleted for *pho8* and expressing mtPho8 (A) or cytPho8 (B). Specific activities of mtPho8 and cytPho8 were normalized to that of the control treated with rapamycin and are given as means ± s.d. (*n*=3). The levels of the mitochondrial markers (Tim23, Aac2 and MPP) and the proteolytic activation of mtPho8 (C) and cytPho8 (D) were determined by SDS-PAGE and western blotting . Bmh2 served as the loading control. (**E**) The indicated strains expressing mtDsRed, and Fis1 or Whi2 were analyzed for mitophagy by confocal fluorescence microscopy after treatment with rapamycin for 7.5 hours to quantify accumulation of mtDsRed in the vacuole. Results are means ± s.d. (*n*=3).

Discussion

In this study, we demonstrate that mitophagy induced by inhibition of TOR signaling is independent of mitochondrial fission. Neither expression of dominant-negative variants of Dnm1 nor deletion of components of the mitochondrial fission machinery resulted in impaired mitophagy. Furthermore, we found that mitochondrial fragmentation due to a block in fusion is not sufficient to trigger mitophagy. These results might help to shed light on the conflicting results published previously. In particular, apparently opposing results were reported for the role of the fission component Dnm1 in mitophagy. In a previous study, downregulation of Mdm38 led to an induction of mitophagy, whereas mitophagy was not observed in a double deletion strain lacking Mdm38 and Dnm1 (Nowikovsky et al., 2007). This result led to the proposal that mitophagy depends on Dnm1 (Nowikovsky et al., 2007). However, a direct role for Dnm1 in this particular case still remains unclear – the extent of mitophagy in the single deletion strain lacking Mdm38 and the effect of impairing Dnm1 function upon downregulation of Mdm38 were not addressed. Another study has shown that mitophagy is reduced by 20–40% in a strain lacking Dnm1, suggesting that mitochondrial fission is crucial for mitophagy in yeast (Kanki et al., 2009a). However, despite the reduction observed under these conditions the data rather confirm that mitophagy is, in principle, efficiently induced in this strain. Furthermore, the same study did not show an impairment of mitophagy upon the lack of any other fission factor, which is inconsistent with the claim that mitochondrial fission impairs mitophagy. In line with our results, a different screen revealed that none of the four components involved in mitochondrial fission affected mitophagy (Okamoto et al., 2009). Another possibility, explaining some of the reported discrepancies discussed above, is that undetected secondary mutations in other genes have occurred. This is not unlikely in light of our results, as we also initially found a specific effect for Fis1, but not for the other fission factors, which we finally demonstrated was caused by a secondary mutation in *WHI2*. In rescue experiments, we demonstrated that it was not the lack of Fis1 that was responsible for the initial defect in mitophagy but rather a suppressor mutation in *WHI2*. In summary, several lines of evidence demonstrate that mitochondrial fission is not strictly required for mitophagy.

This unexpected result seems to put the hypothesis of fission and fusion dynamics acting as a quality control checkpoint for mitochondria into question. However, it is still far from understood how fusion and fission, as well as mitophagy, are initiated or regulated. We cannot rule out the possibility that, under normal growth conditions, basal levels of mitophagy in yeast are triggered in coordination with or as a consequence of mitochondrial fission, similar to the situation in mammalian cells (Twig et al., 2008). Such a low level of steady-state mitophagy might be too little to be detected with the biochemical methods used here. Moreover, we cannot exclude that under a specific condition in which mitochondrial dysfunction is induced, fission promotes degradation of damaged mitochondria. Such an induction of mitophagy might possibly require one or more additional triggers besides fragmentation. In mammalian cells, the induction of mitophagy through recruitment of PARKIN to mitochondria has been shown to depend on the dissipation of the membrane potential (Narendra et al., 2009), suggesting that mitochondrial dysfunction is involved in generating specific signals for mitophagy. In yeast, the induction of mitophagy by mitochondrial dysfunction has only been observed in a few studies (Nowikovsky et al., 2007; Priault et al., 2005). However, drug-induced dissipation of the membrane potential and inhibition of the F_1F_o-ATPase does not lead to an induction of mitophagy in yeast. Furthermore, neither a mitochondrial membrane potential nor the ATP-generating ability of mitochondria is required for rapamycin-induced mitophagy. In future, this and other models of mitochondrial dysfunction need to be investigated in greater detail. In summary, our study does not rule out the possibility that mitochondrial morphology is important for the selection of dysfunctional parts of mitochondria in proliferating cells or that it participates in signaling of a mitochondrial dysfunction to induce mitophagy. However, it shows that mitophagy in yeast does not necessarily require mitochondrial fission, and alternative pathways for mitochondrial quality control by mitophagy need to be considered.

As fission is not required for mitophagy in yeast, how can the sequestration of mitochondrial parts by autophagosomes be accomplished? Kim and colleagues (Kim et al., 2007) reported that mitochondrial fission and autophagosome formation are coordinated events. This means that, during that process, mitochondrial fission might be mediated by the autophagic machinery itself. Recently, organelle-specific mitophagy receptors in yeast and human have been identified, namely Atg32 and NIX, respectively (Kanki et al., 2009b; Novak et al., 2010; Okamoto et al., 2009). The interaction of those proteins with components of the autophagy machinery indicates their involvement in the selection of mitochondria for degradation. It is certainly possible that those and other factors also function in the fission process during autophagosome formation. Future studies will have to dissect whether this is indeed the case and whether mammalian and yeast cells differ in their capacity to separate parts from the mitochondrial network by autophagosome formation. Another possibility as to why mammalian cells but not yeast cells have evolved a dependency on the regular fission machinery could be linked to the size of the mitochondrial tubular network itself. In yeast, the dimensions of mitochondrial tubules are possibly small enough to allow them to be surrounded by autophagosomes. In addition, repeated cell divisions might be sufficient to generate small enough entities. By contrast, in mammalian cells, the larger cell size and the lower frequency of cell divisions (or its absence in post-mitotic tissues) might have led to the dependency on the mitochondrial fission machinery. Moreover, regulating mitochondrial dynamics would create an additional level of regulation for the selective degradation of mitochondria in mammalian cells, which is likely to be of particular importance for post-mitotic cells.

Our data further indicate that regulation of mitophagy in yeast is connected to the stress response and the Ras-PKA signaling pathway. We initially observed an effect on mitophagy in a Δ*fis1* deletion strain, which we demonstrated was caused by a secondary mutation in *WHI2*. This suppressor mutation has been described previously as arising in *fis1* deletion strains and results in an overgrowth phenotype (Cheng et al., 2008). Although in that previous study, the EUROSCARF Δ*caf4* strain was also reported to contain a mutation in *WHI2*, we did not observe a defect in mitophagy in the Δ*caf4* strain used herein. Consistent with this result, our Δ*caf4* strain did not contain a mutation in *WHI2*. So far, very little is known about the cellular function of Whi2. On the basis of previous studies, loss of *WHI2* results in a decreased response to certain stresses; for example, nutrient limitation upon entering into the stationary phase (Radcliffe et al., 1997; Sudbery et al., 1980). This is in line with our observation that loss of Whi2 function leads to a decreased response after inhibition of TOR,

which is known to partially mimic nutrient depletion. We found a direct dependency of mitophagy, and to a lesser extent of autophagy, on Whi2, demonstrating for the first time a role of Whi2 in both processes. Our data further indicate that Whi2 positively modulates autophagic flux. In a previous study, Whi2 was shown to interact physically with the phosphatases Psr1 and Psr2, and the transcription factor Msn2, which regulate the general stress response (Kaida et al., 2002). It is therefore possible that the induction of autophagy and mitophagy is directly or indirectly regulated by the general stress response. In line with this theory, it has been demonstrated that the Msn2-dependent stress response is activated upon inhibition of TOR and nutrient depletion (Beck and Hall, 1999; Gorner et al., 2002). Moreover, it is known that Msn2 is regulated by the Ras-PKA signaling pathway (Gorner et al., 1998). A recent study by Leadsham and colleagues (Leadsham et al., 2009) supports a role for Whi2 in the Ras-PKA signaling pathway, which in turn is known to influence autophagy (Budovskaya et al., 2004; Schmelzle et al., 2004). Interestingly, mitochondria in Δ*whi2* cells were reported to exhibit a reduced membrane potential, to be fragmented and to produce high amounts of reactive oxygen species (ROS) during diauxic shift (Leadsham et al., 2009). The data presented here suggest that these effects could be due to a reduced elimination of damaged mitochondria through mitophagy. In general, our study indicates that TOR signaling, Ras-PKA signaling and the general stress response pathway are linked to mitophagy. It is noteworthy that loss of Whi2 function has a stronger impact on mitophagy than upon autophagy, suggesting that the induction of the two processes might be regulated independently. Future studies will be necessary to decipher the precise roles and the interplay of these signaling pathways on mitophagy and autophagy, and will help to improve our understanding of how mitochondrial quality control is regulated.

Materials and Methods

Yeast strains, plasmids, media and growth conditions

The yeast strains and plasmids used are listed in supplementary material Tables S1 and S2. Single deletion strains were obtained from the EUROSCARF clone collection (BY4742 Mat α; his3Δ1; leu2Δ0; lys2Δ0; ura3Δ0); gene deletion was confirmed by PCR. The mutant *mgm1-5* strain was a gift from Jodi Nunnari (Molecular and Cellular Biology, University of California, Davis, CA). *PHO8* was replaced with a *HIS* cassette amplified from pFA6aHISMX6 using the following primers: 5′-AGACCACAGGGTAGTCAACAGCAGCGGCAACAACGACAAAATGCGC-GTCGTACGCTGCAGGTCGC-3′ and 5′-CGAGATTTCACTTCTTCACGCTA-TAGAATGCACCTAAAACTCGCCATCGATGAATTCGAGCTC-3′. Deletions of *PHO8* were confirmed by western blotting and analysis of the activity of Pho8. The pYX242 cytPho8 and pVT100U cytPho8 plasmids were constructed by amplification of *PHO8* (nucleotide position 181–1701), including an additional start codon, followed by ligation into the *Avr*II and *Mlu*I sites of pYX242 and the *Pst*1 and *Bam*HI sites of pVT100U. For construction of pVT100U mtPho8, the *PHO8* fragment was ligated into the *Kpn*I and *Sac*I sites of pVT100U containing Su9 (nucleotide position 1–207) from *Neurospora crassa* (Westermann and Neupert, 2000). The resulting Su9–pho8 fragment was amplified and cloned into the *Mlu*I and *Sac*I sites of pYX242, resulting in pYX242 mtPho8. For endogenous *FIS1* expression, the gene was amplified from genomic DNA, including 515 bp of the 5′–UTR (untranslated region) and 238 bp of the 3′-UTR of *FIS1*. YPLac33 *WHI2* and pRS313 mtdSRed.T4 were gifts from Marie J. Hardwick (Molecular Microbiology and Immunology, Johns Hopkins University, Baltimore, MD) and Stefan Jakobs (Department of NanoBiophotonics, Max Planck Institute for Biophysical Chemistry, Göttingen, Germany), respectively. GFP–Atg8 including the endogenous promoter of Atg8, kindly provided by Hagai Abeliovich (Institute of Biochemistry, The Hebrew University of Jerusalem, Israel), was cloned into pRS316. The plasmid encoding Whi2–His_9 was constructed by amplifying *WHI2* from genomic DNA (BY4742) and inserting the coding sequence of a His_9 tag, followed by ligation into the *Pvu*II and *Bam*HI sites of pVT100U. Culturing of yeast strains was performed using standard methods (Sherman, 2002) at 30°C. Strains containing plasmids were grown on selective liquid SG medium [2% (v/v) glycerol, 0.1% (w/v) glucose, 0.17% yeast nitrogen base (YNB) supplemented with 5 g/l $(NH_4)_2SO_4$ and amino acids] unless otherwise stated.

Alkaline-phosphatase-based autophagy and mitophagy assay

For monitoring autophagy or mitophagy, strains deleted for *PHO8* were transformed with cytPho8- or mtPho8-expressing plasmids, respectively. The cultures were kept in the exponential growth phase for at least six generations and were then treated with 1 μM rapamycin (LC Laboratories) in DMSO or shifted to liquid SG-N medium [SG without $(NH_4)_2SO_4$]. For determination of the Pho8 enzyme activity, the yeast culture [with an attenuance at 600 nm of ~4] was harvested, washed with ice-cold 0.2 mM PMSF in H_2O and resuspended in 200 μl of lysis buffer (10 mM $MgCl_2$, 0.1 M KAc, 50 mM KCl, 10 nM $ZnSO_4$, 20 mM PIPES pH 7.0, 0.5% Triton X-100 and 1 mM PMSF). The cell suspension was mixed with an equal volume of 0.5-mm glass beads (Roth) and lysed for 10 seconds at 5000 rev./minute in a Precellys 24 cell homogenizer (Bertin Technologies). After mixing with 100 μl of additional lysis buffer, cell lysates were centrifuged at 13,000 ***g*** and the supernatants transferred into a 96-well plate. The protein concentration was determined with the BCA assay (Pierce) according to the manufacturer's instructions at three different dilutions. Pho8 activity was determined by incubation with reaction buffer (40 mM $MgCl_2$, 0.5% Triton X-100, 0.25 M Tris-HCl pH 8.5 and 4 mM *p*-nitrophenylphosphate) for 15 minutes at 37°C for at least two different concentrations. The reaction was stopped with 2 M glycine-NaOH pH 11, and absorption was determined at 405 nm using a Thermo Scientific plate reader. Specific activities are expressed as a percentage normalized to that in the control strain treated with rapamycin for 24 hours. Cell lysates were subjected to SDS-PAGE and western blotting.

Fluorescence microscopy

For mitochondrial morphology analysis, strains were transformed with pHS12 mtDsRedT.3 and the cultures were kept in the exponential growth phase for at least six generations, before being imaged using a Zeiss Axioplan microscope. Pictures were taken with a CCD camera. To visualize mitophagy and autophagy by confocal fluorescence microscopy, strains expressing mtDsRed (pRS313 mtDsRed.T4) and GFP–Atg8 were kept in the exponential growth phase for at least six generations and were then treated with DMSO or 1 μM rapamycin for 7.5 hours. To analyze the mitochondrial membrane potential, cells were stained with 100 nM Rhodamine B hexyl ester perchlorate (Invitrogen) for 15 minutes. Yeast cells were harvested and fixed with 2% low-melting-point agarose (Sigma) before microscopy. Images were taken with a laser-scanning confocal microscope (ECLIPSE TE 2000-E, Nikon), with a 1.49 NA oil immersion lens (APO TIRF 60×, Nikon) and a microscope-integrated intermediate magnification of 1.5-fold. GFP and DsRed were successively excited with an argon laser and a helium-neon laser (GFP: 488 nm excitation, 515 nm detection, 30 nm bandwidth; DsRed: 543 nm excitation, 605 nm detection, 75 nm bandwidth). Background reduction was performed with appropriate saturation levels using software EZ-C1 v. 3.70 (Nikon) and ImageJ. Image stacks for analysis of mitochondrial morphology and quantification of mitophagy were acquired with steps of 0.25 to 0.4 μm per plane in the *z*-direction and a total thickness of 5–7 μm. The acquired stacks were rendered with EZ-C1 software. For quantification of mitophagy, the percentage of cells showing vacuolar accumulation of mtDsRed was calculated. At least three independent experiments were performed for each strain.

Cell fractionation

Cells were harvested and treated with zymolyase to generate spheroplasts, essentially as described previously (Daum et al., 1982). Spheroplasts were homogenized in a glass–teflon homogenizer. After this step, samples representing the total cell extracts were taken. Total cell extracts were centrifuged at 3000 ***g*** for 5 minutes to remove cell debris. For crude separation of mitochondria and cytosol, the cell extract was centrifuged at 11,000 ***g*** for 10 minutes. The mitochondrial pellet was washed twice in HS buffer (20 mM HEPES-KOH pH 7.4, 0.6 M sorbitol and 1 mM PMSF) and stored in liquid nitrogen. To obtain the cytosolic fraction, the supernatant was clarified by centrifugation at 90,000 ***g*** for 30 minutes. Mitochondria were purified on a 60%–55%–44% (w/v) sucrose step gradient at 126,444 ***g*** for 2.30 hours, harvested from the 44%–55% interphase, centrifuged at 11,000 ***g*** for 10 minutes and resuspended in HS buffer. To obtain the vacuolar fraction, the cell extract was separated on a four-step Ficoll gradient and vacuoles were harvested from the 0%–4% (w/v) Ficoll interphase, as described previously (Haas, 1995). Protein concentrations of each fraction were determined by the Bradford assay (Bio-Rad), according to the manufacturer's instructions, and were then mixed with SDS sample buffer and subjected to SDS-PAGE and western blotting using polyclonal antibodies against the indicated organellar marker proteins.

Proteinase K treatment

Mitochondria were diluted to 0.2 μg/μl in HS or HST buffer (HS plus 1% Triton X-100) and treated with 0.1 μg/μl proteinase K for 30 minutes on ice. Proteinase K was inhibited by adding PMSF to a final concentration of 1 mM. Mitochondria were centrifuged at 11,000 ***g***, washed with HS buffer and precipitated with 12% trichloric acid. The samples were centrifuged, washed with acetone, and the dry pellets were resuspended in SDS loading buffer. Samples including an untreated control were subjected to SDS-PAGE and western blotting.

SDS-PAGE and western blotting

Samples with equal amounts of protein were mixed with SDS loading buffer (2% SDS, 10% glycerin, 60 mM Tris-HCl pH 6.8, 0.005% Bromphenol Blue and 5% 2-

mercaptoethanol), separated by SDS-PAGE, transferred onto nitrocellulose membranes and detected by western blotting using rabbit polyclonal antibodies and goat anti-(rabbit Ig) secondary antibodies (Bio-Rad).

We are grateful to Stephane Duvezin-Caubet, Michael Zick, Kai Hell and Walter Neupert for inspiring scientific discussions, and Christiane Kotthoff and Christian Bach for excellent technical assistance. We thank J. Nunnari, H. Abeliovich, S. Jakobs, K. Okamoto, and J. M. Hardwick for kindly providing strains, plasmids and antibodies. This work was supported by the Deutsche Forschungsgemeinschaft DFG project no. RE-1575/1-1 (to A.R. and A.O.), Cluster of Excellence 'Macromolecular Complexes' at the Goethe University Frankfurt DFG project EXC 115 (to A.R.) and the SFB 594 (to A.R. and N.M.).

Supplementary material available online at
http://jcs.biologists.org/cgi/content/full/124/8/1339/DC1

References

Alexander, C., Votruba, M., Pesch, U. E., Thiselton, D. L., Mayer, S., Moore, A., Rodriguez, M., Kellner, U., Leo-Kottler, B., Auburger, G. et al. (2000). OPA1, encoding a dynamin-related GTPase, is mutated in autosomal dominant optic atrophy linked to chromosome 3q28. *Nat. Genet.* **26**, 211-215.

Banerjee, R., Starkov, A. A., Beal, M. F. and Thomas, B. (2009). Mitochondrial dysfunction in the limelight of Parkinson's disease pathogenesis. *Biochim. Biophys. Acta* **1792**, 651-663.

Beck, T. and Hall, M. N. (1999). The TOR signalling pathway controls nuclear localization of nutrient-regulated transcription factors. *Nature* **402**, 689-692.

Bereiter-Hahn, J. and Voth, M. (1994). Dynamics of mitochondria in living cells: shape changes, dislocations, fusion, and fission of mitochondria. *Microsc. Res. Tech.* **27**, 198-219.

Bevis, B. J. and Glick, B. S. (2002). Rapidly maturing variants of the Discosoma red fluorescent protein (DsRed). *Nat. Biotechnol.* **20**, 83-87.

Budovskaya, Y. V., Stephan, J. S., Reggiori, F., Klionsky, D. J. and Herman, P. K. (2004). The Ras/cAMP-dependent protein kinase signaling pathway regulates an early step of the autophagy process in Saccharomyces cerevisiae. *J. Biol. Chem.* **279**, 20663-20671.

Campbell, C. L. and Thorsness, P. E. (1998). Escape of mitochondrial DNA to the nucleus in yme1 yeast is mediated by vacuolar-dependent turnover of abnormal mitochondrial compartments. *J. Cell Sci.* **111**, 2455-2464.

Carrera, A. C. (2004). TOR signaling in mammals. *J. Cell Sci.* **117**, 4615-4616.

Cerveny, K. L., McCaffery, J. M. and Jensen, R. E. (2001). Division of mitochondria requires a novel DMN1-interacting protein, Net2p. *Mol. Biol. Cell* **12**, 309-321.

Chen, Y., McMillan-Ward, E., Kong, J., Israels, S. J. and Gibson, S. B. (2007). Mitochondrial electron-transport-chain inhibitors of complexes I and II induce autophagic cell death mediated by reactive oxygen species. *J. Cell Sci.* **120**, 4155-4166.

Cheng, W. C., Teng, X., Park, H. K., Tucker, C. M., Dunham, M. J. and Hardwick, J. M. (2008). Fis1 deficiency selects for compensatory mutations responsible for cell death and growth control defects. *Cell Death Differ.* **15**, 1838-1846.

Daum, G., Bohni, P. C. and Schatz, G. (1982). Import of proteins into mitochondria. Cytochrome b2 and cytochrome c peroxidase are located in the intermembrane space of yeast mitochondria. *J. Biol. Chem.* **257**, 13028-13033.

Delettre, C., Lenaers, G., Griffoin, J. M., Gigarel, N., Lorenzo, C., Belenguer, P., Pelloquin, L., Grosgeorge, J., Turc-Carel, C., Perret, E. et al. (2000). Nuclear gene OPA1, encoding a mitochondrial dynamin-related protein, is mutated in dominant optic atrophy. *Nat. Genet.* **26**, 207-210.

Ding, W. X., Ni, H. M., Li, M., Liao, Y., Chen, X., Stolz, D. B., Dorn, G. W., 2nd. and Yin, X. M. (2010). Nix is critical to two distinct phases of mitophagy, reactive oxygen species-mediated autophagy induction and Parkin-ubiquitin-p62-mediated mitochondrial priming. *J. Biol. Chem.* **285**, 27879-27890.

Duvezin-Caubet, S., Jagasia, R., Wagener, J., Hofmann, S., Trifunovic, A., Hansson, A., Chomyn, A., Bauer, M. F., Attardi, G., Larsson, N. G. et al. (2006). Proteolytic processing of OPA1 links mitochondrial dysfunction to alterations in mitochondrial morphology. *J. Biol. Chem.* **281**, 37972-37979.

Exner, N., Treske, B., Paquet, D., Holmstrom, K., Schiesling, C., Gispert, S., Carballo-Carbajal, I., Berg, D., Hoepken, H. H., Gasser, T. et al. (2007). Loss-of-function of human PINK1 results in mitochondrial pathology and can be rescued by parkin. *J. Neurosci.* **27**, 12413-12418.

Fritz, S., Rapaport, D., Klanner, E., Neupert, W. and Westermann, B. (2001). Connection of the mitochondrial outer and inner membranes by Fzo1 is critical for organellar fusion. *J. Cell Biol.* **152**, 683-692.

Geisler, S., Holmstrom, K. M., Skujat, D., Fiesel, F. C., Rothfuss, O. C., Kahle, P. J. and Springer, W. (2010). PINK1/Parkin-mediated mitophagy is dependent on VDAC1 and p62/SQSTM1. *Nat. Cell Biol.* **12**, 119-131.

Gorner, W., Durchschlag, E., Martinez-Pastor, M. T., Estruch, F., Ammerer, G., Hamilton, B., Ruis, H. and Schuller, C. (1998). Nuclear localization of the C2H2 zinc finger protein Msn2p is regulated by stress and protein kinase A activity. *Genes Dev.* **12**, 586-597.

Gorner, W., Durchschlag, E., Wolf, J., Brown, E. L., Ammerer, G., Ruis, H. and Schuller, C. (2002). Acute glucose starvation activates the nuclear localization signal of a stress-specific yeast transcription factor. *EMBO J.* **21**, 135-144.

Griffin, E. E., Graumann, J. and Chan, D. C. (2005). The WD40 protein Caf4p is a component of the mitochondrial fission machinery and recruits Dnm1p to mitochondria. *J. Cell Biol.* **170**, 237-248.

Haas, A. (1995). A quantitative assay to measure homotypic vacuole fusion in vitro. *Methods Cell Sci.* **17**, 283-294.

Herlan, M., Vogel, F., Bornhövd, C., Neupert, W. and Reichert, A. S. (2003). Processing of Mgm1 by the rhomboid-type protease Pcp1 is required for maintenance of mitochondrial morphology and of mitochondrial DNA. *J. Biol. Chem.* **278**, 27781-27788.

Herlan, M., Bornhövd, C., Hell, K., Neupert, W. and Reichert, A. S. (2004). Alternative topogenesis of Mgm1 and mitochondrial morphology depend on ATP and a functional import motor. *J. Cell Biol.* **165**, 167-173.

Hermann, G. J., Thatcher, J. W., Mills, J. P., Hales, K. G., Fuller, M. T., Nunnari, J. and Shaw, J. M. (1998). Mitochondrial fusion in yeast requires the transmembrane GTPase Fzo1p. *J. Cell Biol.* **143**, 359-373.

Huang, J. and Klionsky, D. J. (2007). Autophagy and human disease. *Cell Cycle* **6**, 1837-1849.

Jakobs, S., Schauss, A. C. and Hell, S. W. (2003). Photoconversion of matrix targeted GFP enables analysis of continuity and intermixing of the mitochondrial lumen. *FEBS Lett.* **554**, 194-200.

Kaida, D., Yashiroda, H., Toh-e, A. and Kikuchi, Y. (2002). Yeast Whi2 and Psr1-phosphatase form a complex and regulate STRE-mediated gene expression. *Genes Cells* **7**, 543-552.

Kanki, T. and Klionsky, D. J. (2008). Mitophagy in yeast occurs through a selective mechanism. *J. Biol. Chem.* **283**, 32386-32393.

Kanki, T., Wang, K., Baba, M., Bartholomew, C. R., Lynch-Day, M. A., Du, Z., Geng, J., Mao, K., Yang, Z., Yen, W. L. et al. (2009a). A genomic screen for yeast mutants defective in selective mitochondria autophagy. *Mol. Biol. Cell* **20**, 4730-4738.

Kanki, T., Wang, K., Cao, Y., Baba, M. and Klionsky, D. J. (2009b). Atg32 is a mitochondrial protein that confers selectivity during mitophagy. *Dev. Cell* **17**, 98-109.

Kim, I., Rodriguez-Enriquez, S. and Lemasters, J. J. (2007). Selective degradation of mitochondria by mitophagy. *Arch. Biochem. Biophys.* **462**, 245-253.

Kim, J., Huang, W. P. and Klionsky, D. J. (2001). Membrane recruitment of Aut7p in the autophagy and cytoplasm to vacuole targeting pathways requires Aut1p, Aut2p, and the autophagy conjugation complex. *J. Cell Biol.* **152**, 51-64.

Kim, J., Huang, W. P., Stromhaug, P. E. and Klionsky, D. J. (2002). Convergence of multiple autophagy and cytoplasm to vacuole targeting components to a perivacuolar membrane compartment prior to de novo vesicle formation. *J. Biol. Chem.* **277**, 763-773.

Kissova, I., Deffieu, M., Manon, S. and Camougrand, N. (2004). Uth1p is involved in the autophagic degradation of mitochondria. *J. Biol. Chem.* **279**, 39068-39074.

Kissova, I., Salin, B., Schaeffer, J., Bhatia, S., Manon, S. and Camougrand, N. (2007). Selective and non-selective autophagic degradation of mitochondria in yeast. *Autophagy* **3**, 329-336.

Klionsky, D. J., Cregg, J. M., Dunn, W. A., Jr, Emr, S. D., Sakai, Y., Sandoval, I. V., Sibirny, A., Subramani, S., Thumm, M., Veenhuis, M. et al. (2003). A unified nomenclature for yeast autophagy-related genes. *Dev. Cell* **5**, 539-545.

Krebiehl, G., Ruckerbauer, S., Burbulla, L. F., Kieper, N., Maurer, B., Waak, J., Wolburg, H., Gizatullina, Z., Gellerich, F. N., Woitalla, D. et al. (2010). Reduced basal autophagy and impaired mitochondrial dynamics due to loss of Parkinson's disease-associated protein DJ-1. *PLoS One* **5**, e9367.

Leadsham, J. E., Miller, K., Ayscough, K. R., Colombo, S., Martegani, E., Sudbery, P. and Gourlay, C. W. (2009). Whi2p links nutritional sensing to actin-dependent Ras-cAMP-PKA regulation and apoptosis in yeast. *J. Cell Sci.* **122**, 706-715.

Legros, F., Lombes, A., Frachon, P. and Rojo, M. (2002). Mitochondrial fusion in human cells is efficient, requires the inner membrane potential, and is mediated by mitofusins. *Mol. Biol. Cell* **13**, 4343-4354.

Lyamzaev, K. G., Pletjushkina, O. Y., Saprunova, V. B., Bakeeva, L. E., Chernyak, B. V. and Skulachev, V. P. (2004). Selective elimination of mitochondria from living cells induced by inhibitors of bioenergetic functions. *Biochem. Soc. Trans.* **32**, 1070-1071.

Meeusen, S., McCaffery, J. M. and Nunnari, J. (2004). Mitochondrial fusion intermediates revealed in vitro. *Science* **305**, 1747-1752.

Mortensen, M., Ferguson, D. J., Edelmann, M., Kessler, B., Morten, K. J., Komatsu, M. and Simon, A. K. (2010). Loss of autophagy in erythroid cells leads to defective removal of mitochondria and severe anemia in vivo. *Proc. Natl. Acad. Sci. USA* **107**, 832-837.

Mozdy, A. D., McCaffery, J. M. and Shaw, J. M. (2000). Dnm1p GTPase-mediated mitochondrial fission is a multi-step process requiring the novel integral membrane component Fis1p. *J. Cell Biol.* **151**, 367-380.

Narendra, D., Tanaka, A., Suen, D. F. and Youle, R. J. (2009). Parkin-induced mitophagy in the pathogenesis of Parkinson disease. *Autophagy* **5**, 706-708.

Narendra, D. P., Jin, S. M., Tanaka, A., Suen, D. F., Gautier, C. A., Shen, J., Cookson, M. R. and Youle, R. J. (2010). PINK1 is selectively stabilized on impaired mitochondria to activate Parkin. *PLoS Biol.* **8**, e1000298.

Naylor, K., Ingerman, E., Okreglak, V., Marino, M., Hinshaw, J. E. and Nunnari, J. (2006). Mdv1 interacts with assembled dnm1 to promote mitochondrial division. *J. Biol. Chem.* **281**, 2177-2183.

Nice, D. C., Sato, T. K., Stromhaug, P. E., Emr, S. D. and Klionsky, D. J. (2002). Cooperative binding of the cytoplasm to vacuole targeting pathway proteins, Cvt13 and Cvt20, to phosphatidylinositol 3-phosphate at the pre-autophagosomal structure is required for selective autophagy. *J. Biol. Chem.* **277**, 30198-30207.

Niemann, A., Ruegg, M., La Padula, V., Schenone, A. and Suter, U. (2005). Ganglioside-induced differentiation associated protein 1 is a regulator of the mitochondrial network: new implications for Charcot-Marie-Tooth disease. *J. Cell Biol.* **170**, 1067-1078.

Noda, T. and Ohsumi, Y. (1998). Tor, a phosphatidylinositol kinase homologue, controls autophagy in yeast. *J. Biol. Chem.* **273**, 3963-3966.

Noda, T., Matsuura, A., Wada, Y. and Ohsumi, Y. (1995). Novel system for monitoring autophagy in the yeast Saccharomyces cerevisiae. *Biochem. Biophys. Res. Commun.* **210**, 126-132.

Novak, I., Kirkin, V., McEwan, D. G., Zhang, J., Wild, P., Rozenknop, A., Rogov, V., Lohr, F., Popovic, D., Occhipinti, A. et al. (2010). Nix is a selective autophagy receptor for mitochondrial clearance. *EMBO Rep.* **11**, 45-51.

Nowikovsky, K., Reipert, S., Devenish, R. J. and Schweyen, R. J. (2007). Mdm38 protein depletion causes loss of mitochondrial K+/H+ exchange activity, osmotic swelling and mitophagy. *Cell Death Differ.* **14**, 1647-1656.

Nunnari, J., Marshall, W. F., Straight, A., Murray, A., Sedat, J. W. and Walter, P. (1997). Mitochondrial transmission during mating in Saccharomyces cerevisiae is determined by mitochondrial fusion and fission and the intramitochondrial segregation of mitochondrial DNA. *Mol. Biol. Cell* **8**, 1233-1242.

Okamoto, K., Kondo-Okamoto, N. and Ohsumi, Y. (2009). Mitochondria-anchored receptor Atg32 mediates degradation of mitochondria via selective autophagy. *Dev. Cell* **17**, 87-97.

Otsuga, D., Keegan, B. R., Brisch, E., Thatcher, J. W., Hermann, G. J., Bleazard, W. and Shaw, J. M. (1998). The dynamin-related GTPase, Dnm1p, controls mitochondrial morphology in yeast. *J. Cell Biol.* **143**, 333-349.

Priault, M., Salin, B., Schaeffer, J., Vallette, F. M., di Rago, J. P. and Martinou, J. C. (2005). Impairing the bioenergetic status and the biogenesis of mitochondria triggers mitophagy in yeast. *Cell Death Differ.* **12**, 1613-1621.

Radcliffe, P., Trevethick, J., Tyers, M. and Sudbery, P. (1997). Deregulation of CLN1 and CLN2 in the Saccharomyces cerevisiae whi2 mutant. *Yeast* **13**, 707-715.

Rapaport, D., Brunner, M., Neupert, W. and Westermann, B. (1998). Fzo1p is a mitochondrial outer membrane protein essential for the biogenesis of functional mitochondria in Saccharomyces cerevisiae. *J. Biol. Chem.* **273**, 20150-20155.

Sandoval, H., Thiagarajan, P., Dasgupta, S. K., Schumacher, A., Prchal, J. T., Chen, M. and Wang, J. (2008). Essential role for Nix in autophagic maturation of erythroid cells. *Nature* **454**, 232-235.

Schauss, A. C., Bewersdorf, J. and Jakobs, S. (2006). Fis1p and Caf4p, but not Mdv1p, determine the polar localization of Dnm1p clusters on the mitochondrial surface. *J. Cell Sci.* **119**, 3098-3106.

Schmelzle, T., Beck, T., Martin, D. E. and Hall, M. N. (2004). Activation of the RAS/cyclic AMP pathway suppresses a TOR deficiency in yeast. *Mol. Cell. Biol.* **24**, 338-351.

Schweers, R. L., Zhang, J., Randall, M. S., Loyd, M. R., Li, W., Dorsey, F. C., Kundu, M., Opferman, J. T., Cleveland, J. L., Miller, J. L. et al. (2007). NIX is required for programmed mitochondrial clearance during reticulocyte maturation. *Proc. Natl. Acad. Sci. USA* **104**, 19500-19505.

Sesaki, H. and Jensen, R. E. (1999). Division versus fusion: Dnm1p and Fzo1p antagonistically regulate mitochondrial shape. *J. Cell Biol.* **147**, 699-706.

Sesaki, H. and Jensen, R. E. (2001). UGO1 encodes an outer membrane protein required for mitochondrial fusion. *J. Cell Biol.* **152**, 1123-1134.

Sesaki, H. and Jensen, R. E. (2004). Ugo1p links the Fzo1p and Mgm1p GTPases for mitochondrial fusion. *J. Biol. Chem.* **279**, 28298-28303.

Sesaki, H., Southard, S. M., Yaffe, M. P. and Jensen, R. E. (2003). Mgm1p, a dynamin-related GTPase, is essential for fusion of the mitochondrial outer membrane. *Mol. Biol. Cell* **14**, 2342-2356.

Sherman, F. (2002). Getting started with yeast. *Methods Enzymol.* **350**, 3-41.

Sikorski, R. S. and Hieter, P. (1989). A system of shuttle vectors and yeast host strains designed for efficient manipulation of DNA in Saccharomyces cerevisiae. *Genetics* **122**, 19-27.

Sudbery, P. E., Goodey, A. R. and Carter, B. L. (1980). Genes which control cell proliferation in the yeast Saccharomyces cerevisiae. *Nature* **288**, 401-404.

Tal, R., Winter, G., Ecker, N., Klionsky, D. J. and Abeliovich, H. (2007). Aup1p, a yeast mitochondrial protein phosphatase homolog, is required for efficient stationary phase mitophagy and cell survival. *J. Biol. Chem.* **282**, 5617-5624.

Tieu, Q. and Nunnari, J. (2000). Mdv1p is a WD repeat protein that interacts with the dynamin-related GTPase, Dnm1p, to trigger mitochondrial division. *J. Cell Biol.* **151**, 353-366.

Twig, G., Elorza, A., Molina, A. J., Mohamed, H., Wikstrom, J. D., Walzer, G., Stiles, L., Haigh, S. E., Katz, S., Las, G. et al. (2008). Fission and selective fusion govern mitochondrial segregation and elimination by autophagy. *EMBO J.* **27**, 433-446.

Vernet, T., Dignard, D. and Thomas, D. Y. (1987). A family of yeast expression vectors containing the phage f1 intergenic region. *Gene* **52**, 225-233.

Westermann, B. and Neupert, W. (2000). Mitochondria-targeted green fluorescent proteins: convenient tools for the study of organelle biogenesis in Saccharomyces cerevisiae. *Yeast* **16**, 1421-1427.

Wong, E. D., Wagner, J. A., Gorsich, S. W., McCaffery, J. M., Shaw, J. M. and Nunnari, J. (2000). The dynamin-related GTPase, Mgm1p, is an intermembrane space protein required for maintenance of fusion competent mitochondria. *J. Cell Biol.* **151**, 341-352.

Wong, E. D., Wagner, J. A., Scott, S. V., Okreglak, V., Holewinske, T. J., Cassidy-Stone, A. and Nunnari, J. (2003). The intramitochondrial dynamin-related GTPase, Mgm1p, is a component of a protein complex that mediates mitochondrial fusion. *J. Cell Biol.* **160**, 303-311.

Yang, Y., Ouyang, Y., Yang, L., Beal, M. F., McQuibban, A., Vogel, H. and Lu, B. (2008). Pink1 regulates mitochondrial dynamics through interaction with the fission/fusion machinery. *Proc. Natl. Acad. Sci. USA* **105**, 7070-7075.

Yang, Z. and Klionsky, D. J. (2009). An overview of the molecular mechanism of autophagy. *Curr. Top. Microbiol. Immunol.* **335**, 1-32.

Yorimitsu, T. and Klionsky, D. J. (2005). Atg11 links cargo to the vesicle-forming machinery in the cytoplasm to vacuole targeting pathway. *Mol. Biol. Cell* **16**, 1593-1605.

Zuchner, S., Mersiyanova, I. V., Muglia, M., Bissar-Tadmouri, N., Rochelle, J., Dadali, E. L., Zappia, M., Nelis, E., Patitucci, A., Senderek, J. et al. (2004). Mutations in the mitochondrial GTPase mitofusin 2 cause Charcot-Marie-Tooth neuropathy type 2A. *Nat. Genet.* **36**, 449-451.

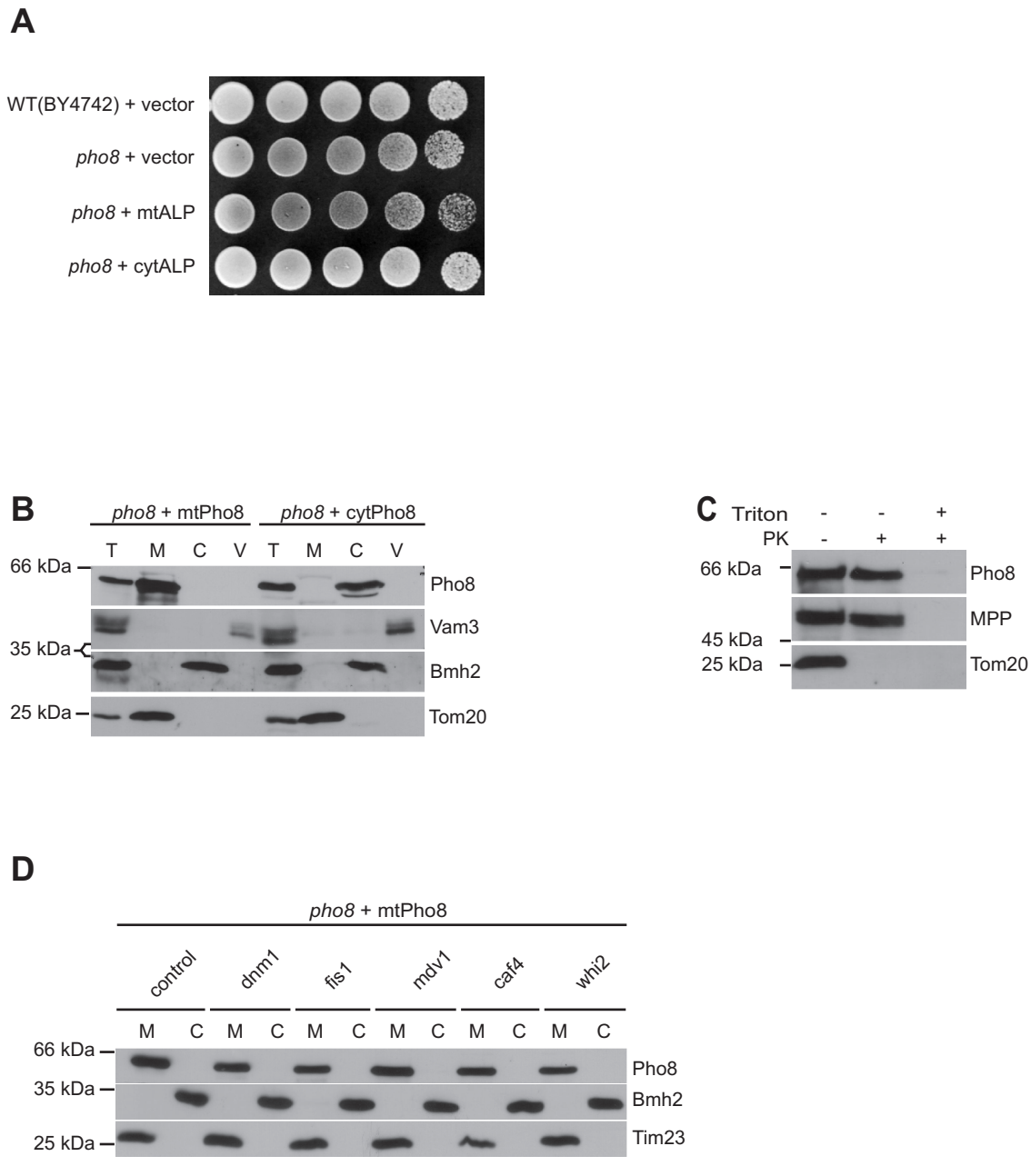
A
WT(BY4742) + vector
pho8 + vector
pho8 + mtALP
pho8 + cytALP
B
pho8 + mtPho8
pho8 + cytPho8
T M C V T M C V
66 kDa
35 kDa
25 kDa
Pho8
Vam3
Bmh2
Tom20
C
Triton - - +
PK - + +
66 kDa
45 kDa
25 kDa
Pho8
MPP
Tom20
D
pho8 + mtPho8
control
dnm1
fis1
mdv1
caf4
whi2
M C M C M C M C M C M C
66 kDa
35 kDa
25 kDa
Pho8
Bmh2
Tim23

A

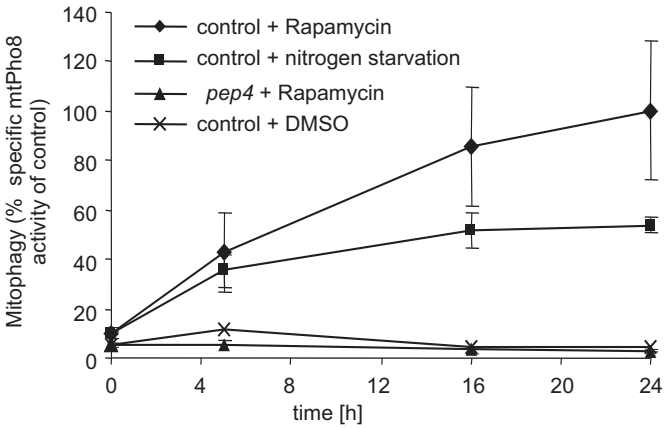
Mitophagy (% specific mtPho8 activity of control)
140
120
100
80
60
40
20
0
0
4
8
12
16
20
24
time [h]
control + Rapamycin
control + nitrogen starvation
pep4 + Rapamycin
control + DMSO

B

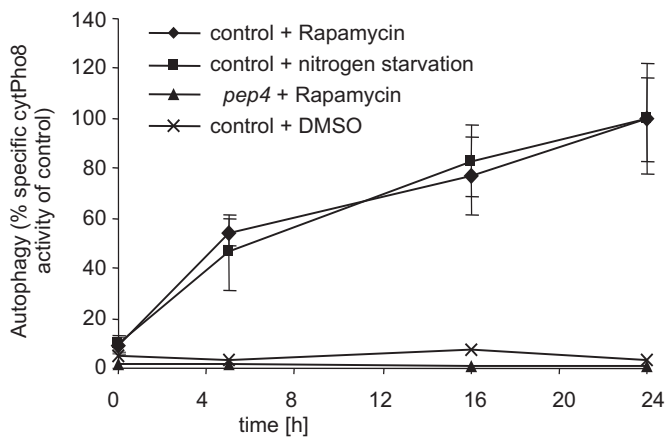
Autophagy (% specific cytPho8 activity of control)
140
120
100
80
60
40
20
0
0
4
8
12
16
20
24
time [h]
control + Rapamycin
control + nitrogen starvation
pep4 + Rapamycin
control + DMSO

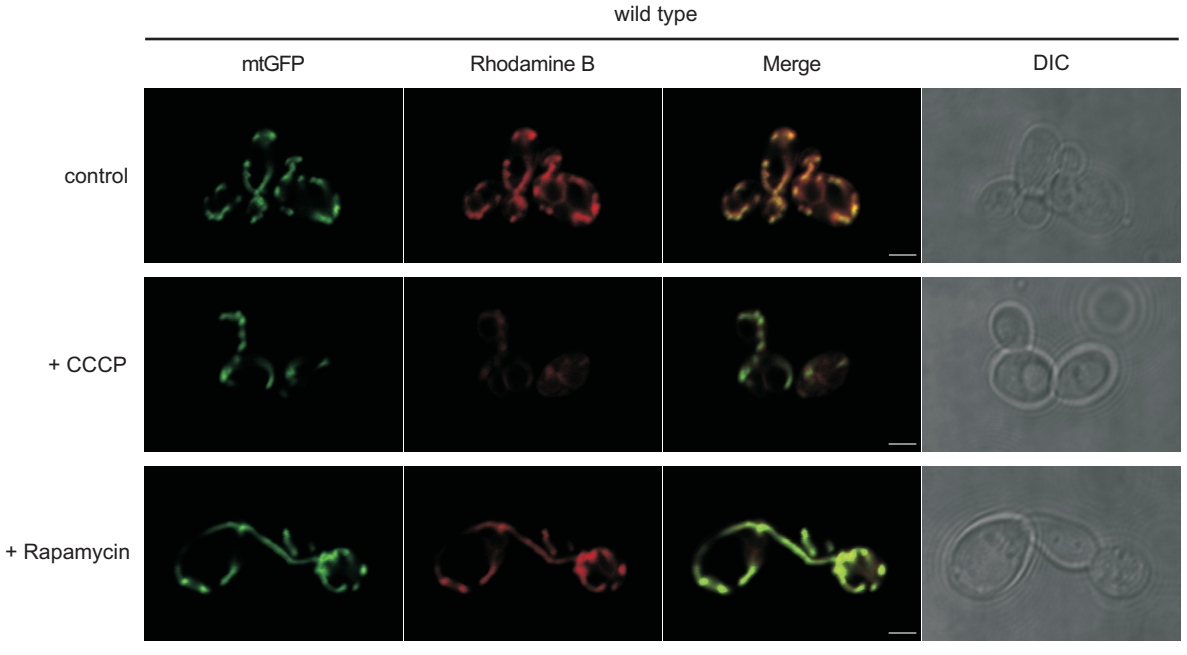
wild type
mtGFP
Rhodamine B
Merge
DIC
control
+ CCCP
+ Rapamycin

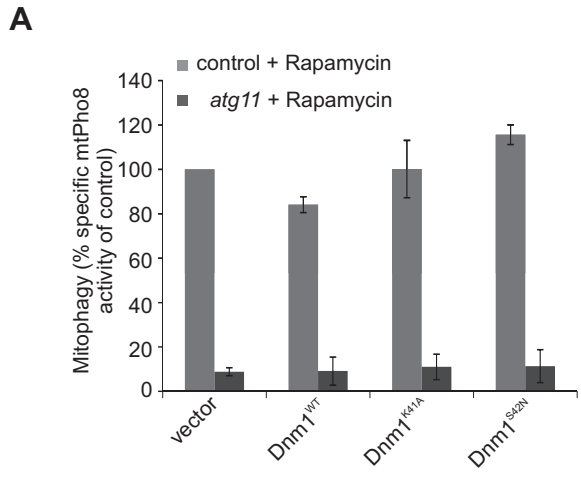
A
control + Rapamycin
atg11 + Rapamycin
Mitophagy (% specific mtPho8 activity of control)
140
120
100
80
60
40
20
0
vector
Dnm1WT
Dnm1K41A
Dnm1S42N

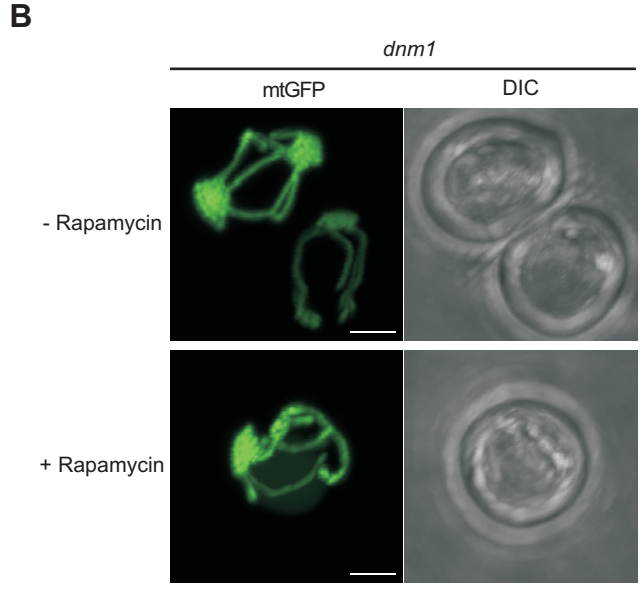
B
dnm1
mtGFP
DIC
- Rapamycin
+ Rapamycin

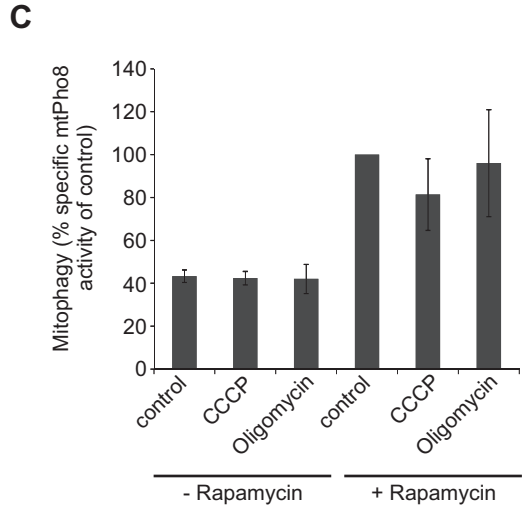
C
Mitophagy (% specific mtPho8 activity of control)
140
120
100
80
60
40
20
0
control
CCCP
Oligomycin
control
CCCP
Oligomycin
- Rapamycin
+ Rapamycin

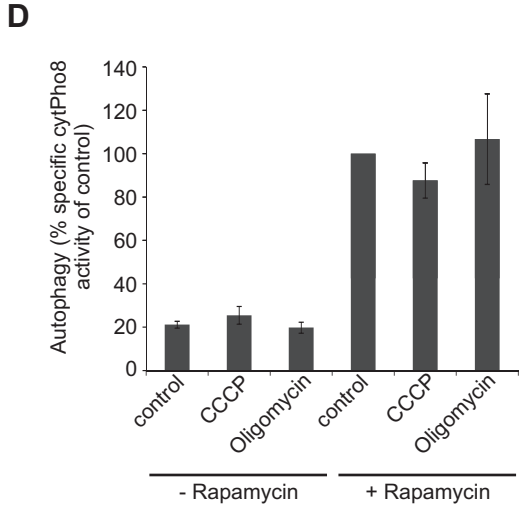
D
Autophagy (% specific cytPho8 activity of control)
140
120
100
80
60
40
20
0
control
CCCP
Oligomycin
control
CCCP
Oligomycin
- Rapamycin
+ Rapamycin

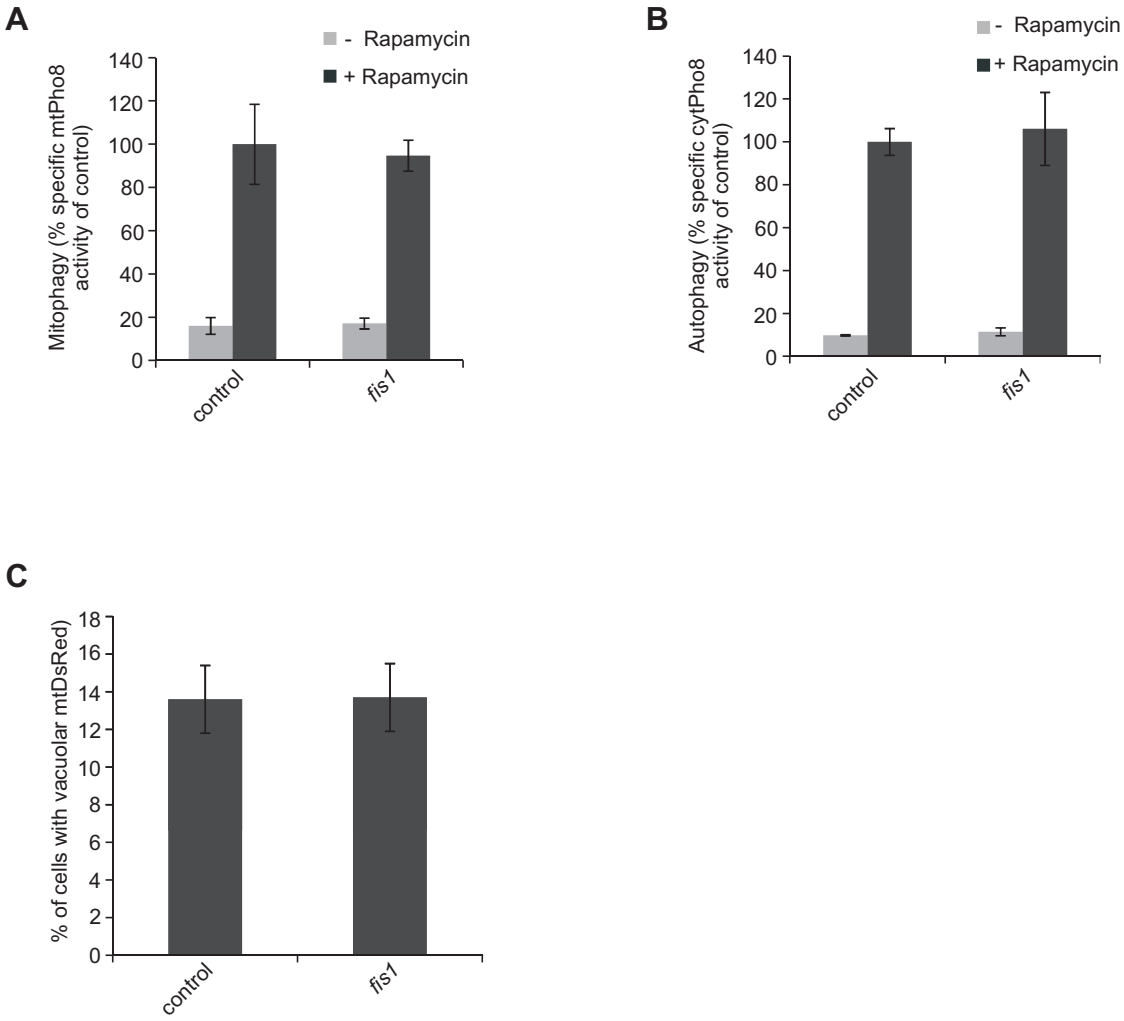
A
- Rapamycin
+ Rapamycin
Mitophagy (% specific mtPho8 activity of control)
140
120
100
80
60
40
20
0
control
fis1
B
- Rapamycin
+ Rapamycin
Autophagy (% specific cytPho8 activity of control)
140
120
100
80
60
40
20
0
control
fis1
C
% of cells with vacuolar mtDsRed)
18
16
14
12
10
8
6
4
2
0
control
fis1

Table S1. Yeast strains used in this study

Name	Genotype	Source
NM201	w303 Matα *ade2-1; his3-11,15; leu2,112; trp1; ura23-53; can1-100*	
NM205	w303 Matα *pho8::HIS3* [pHS12 mtDsRed.T3] [pYX242mtPho8]	This study
NM211	BY4742 Matα *his3Δ1 ; leu2Δ0 ; lys2Δ0 ; Ura3Δ0*	
NM214	BY4742 Matα [pRS316 GFP-Atg8] [pRS323 mtDsRed.T4]	This study
NM215	w303 Mata *mgm1-5 G408D*	Wong et al. 2000
NM218	w303 Mata *mgm1-5 pho8::HIS3* [pHS12 mtdSRed.T3] [pVT100U mtPho8]	This study
NM225	BY4742 Matα *pho8::kanMX4* [pRS323 mtDsRed.T4] [pRS316 GFP-Atg8]	This study
NM021	BY4742 Matα *pho8::kanMX4* [pVT100U mtGFP] [pYX242 mtPho8]	This study
NM022	BY4742 Matα *pho8::kanMX4* [pVT100U mtGFP] [pYX242 cytPho8]	This study
NM 6-1	BY4742 Matα *pho8::kanMX4* [Yep213] [pVT100U mtPho8]	This study
NM380	BY4742 Matα *pho8::kanMX4* [Yep213] [pVT100U cytPho8]	This study
NM 6	BY4742 Matα *pho8::kanMX4* [Yep213 Dnm1a] [pVT100U mtPho8]	This study
NM378	BY4742 Matα *pho8::kanMX4* [Yep213 Dnm1a] [pVT100U cytPho8]	This study
NM233	BY4742 Matα *pho8::kanMX4* [Yep213 Dnm1 K41A] [pVT100U mtPho8]	This study
NM379	BY4742 Matα *pho8::kanMX4* [Yep213 Dnm1 K41A] [pVT100U cytPho8]	This study
NM234	BY4742 Matα *pho8::kanMX4* [Yep213 Dnm1 S42N] [pVT100U mtPho8]	This study
NM235	BY4742 Matα *pho8::kanMX4* [Yep213 Dnm1 S42N] [pVT100U cytPho8]	This study
NM246	BY4742 Matα *dnm1::kanMX4* [pRS316 GFP-Atg8] [pRS323 mtDsRed.T4]	This study
NM070	BY4742 Matα *dnm1::kanMX4 pho8::HIS3* [pVT100U mtGFP] [pYX242 mtPho8]	This study
NM071	BY4742 Matα *dnm1::kanMX4 pho8::HIS3* [pVT100U mtGFP] [pYX242 cytPho8]	This study
NM261	BY4742 Matα *fis1::kanMX4 whi2-1* [pRS316 GFP-Atg8] [pRS323 mtDsRed.T4]	This study
R-771	BY4742 Matα *fis1::kanMX4 whi2-2* [pRS323 mtDsRed.T4] [pRS416]	This study
R-772	BY4742 Matα *fis1::kanMX4 whi2-2* [pRS323 mtDsRed.T4] [pRS416 Fis1]	This study
R-773	BY4742 Matα *fis1::kanMX4 whi2-2* [pRS323 mtDsRed.T4] [YPlac33 Whi2]	This study
NM044	BY4742 Matα *fis1::kanMX4 whi2-1 pho8::HIS3* [pVT100U mtGFP] [pYX242 mtPho8]	This study
NM043	BY4742 Matα *fis1::kanMX4 whi2-1 pho8::HIS3* [pVT100U mtGFP] [pYX242 cytPho8]	This study
NM091	BY4742 Matα *fis1::kanMX4 whi2-1 pho8::HIS3* [pRS416 Fis1] [pYX242 mtPho8]	This study
NM092	BY4742 Matα *fis1::kanMX4 whi2-1 pho8::HIS3* [pRS416 Fis1] [pYX242 cytPho8]	This study
NM095	BY4742 Matα *fis1::kanMX4 whi2-1 pho8::HIS3* [pRS416] [pYX242 mtPho8]	This study
NM096	BY4742 Matα *fis1::kanMX4 whi2-1 pho8::HIS3* [pRS416] [pYX242 cytPho8]	This study
NM093	BY4742 Matα *fis1::kanMX4 whi2-1 pho8::HIS3* [YPLac33 Whi2] [pYX242 mtPho8]	This study
NM094	BY4742 Matα *fis1::kanMX4 whi2-1 pho8::HIS3* [YPLac33 Whi2] [pYX242 cytPho8]	This study
NM297	BY4742 Matα *atg8::kanMX4 pho8::HIS3* [pVT100U mtGFP] [pYX242 mtPho8]	This study
NM298	BY4742 Matα *atg8::kanMX4 pho8::HIS3* [pVT100U mtGFP] [pYX242 cytPho8]	This study
NM327	BY4742 Matα *mdv1::kanMX4* [pRS316 GFP-Atg8] [pRS323 mtDsRed.T4]	This study
NM03	BY4742 Matα *mdv1::kanMX4 pho8::HIS3* [pVT100U mtGFP] [pYX242 mtPho8]	This study
NM04	BY4742 Matα *mdv1::kanMX4 pho8::HIS3* [pVT100U mtGFP] [pYX242 cytPho8]	This study
NM375	BY4742 Matα *caf4::kanMX4* [pRS316 GFP-Atg8] [pRS323 mtDsRed.T4]	This study
NM050	BY4742 Matα *caf4::kanMX4 pho8::HIS3* [pVT100U mtGFP] [pYX242 mtPho8]	This study
NM333	BY4742 Matα *caf4::kanMX4 pho8::HIS3* [pVT100U mtGFP] [pYX242 cytPho8]	This study
NM344	BY4742 Matα *atg11::kanMX4* [pRS316 GFP-Atg8] [pRS323 mtDsRed.T4]	This study
NM346	BY4742 Matα *atg11::kanMX4 pho8::HIS3* [pVT100U mtGFP] [pYX242mtPho8]	This study
NM347	BY4742 Matα *atg11::kanMX4 pho8::HIS3* [pVT100U mtGFP] [pYX242 cytPho8]	This study
NM350	BY4742 Matα *atg20::kanMX4 pho8::HIS3* [pVT100U mtGFP] [pYX242 mtPho8]	This study
NM351	BY4742 Matα *atg20::kanMX4 pho8::HIS3* [pVT100U mtGFP] [pYX242 cytPho8]	This study
NM354	BY4742 Matα *atg24::kanMX4 pho8::HIS3* [pVT100U mtGFP] [pYX242 mtPho8]	This study
NM355	BY4742 Matα *atg24::kanMX4 pho8::HIS3* [pVT100U mtGFP] [pYX242 cytPho8]	This study
NM023	BY4742 Matα *pep4::kanMX4 pho8::HIS3* [pVT100U mtGFP] [pYX242 mtPho8]	This study
NM024	BY4742 Matα *pep4::kanMX4 pho8::HIS3* [pVT100U mtGFP] [pYX242 cytPho8]	This study
NM365	BY4742 Matα *whi2::kanMX4* [pRS316 GFP-Atg8 [pRS323 mtdSRed.T4]	This study
NM041	BY4742 Matα *whi2::kanMX4 pho8::HIS3* [pVT100U mtGFP] [pYX242 mtPho8]	This study
NM042	BY4742 Matα *whi2::kanMX4 pho8::HIS3* [pVT100U mtGFP] [pYX242 cytPho8]	This study
NM064	BY4742 Matα *whi2::kanMX4 pho8::HIS3* [YPLac33 Whi2] [pYX242 mtPho8]	This study
NM065	BY4742 Matα *whi2::kanMX4 pho8::HIS3* [YPLac33 Whi2] [pYX242 cytPho8]	This study
NM101	BY4742 Matα *whi2::kanMX4 pho8::HIS3* [pRS416] [pYX242 mtPho8]	This study
NM102	BY4742 Matα *whi2::kanMX4 pho8::HIS3* [pRS416] [pYX242 cytPho8]	This study
R-952	BY4742 Matα *fis1::kanMX4 whi2-2* [pRS323 mtDsRed.T4] [pRS416]	This study
R-954	BY4742 Matα *fis1::kanMX4 whi2-2* [pRS323 mtDsRed.T4] [YPlac33 Whi2]	This study
NM409	W303 Matα *fis1::KanMX4 pho8::HIS3* [pVT100U mtGFP] [pYX242 mtPho8]	This study
NM407	W303 Matα *fis1::KanMX4 pho8::HIS3* [pVT100U mtGFP] [pYX242 cytPho8]	This study
R-1192	W303 Matα *fis1::KanMX4 pho8::HIS3* [pRS316 GFP-Atg8] [pHS12 mtDsRed.T3]	This study

R-1288	BY4742 Matα *whi2::kanMX4* [pRS313 GFP-Atg8] [pVT100U]	This study
R-1287	BY4742 Matα *whi2::kanMX4* [pRS313 GFP-Atg8] [pVT100U Whi2-His]	This study
R-1276	BY4742 Matα [pYX242]	This study
R-1277	BY4742 Matα *pho8::kanMX4* [pYX242]	This study
R-1278	BY4742 Matα *pho8::kanMX4* [pYX242 mtPho8]	This study
R-1279	BY4742 Matα *pho8*::*kanMX4* [pYX242 cytPho8]	This study
NM453	BY4742 Matα [pVT100U mtGFP]	This study

Table S2: Plasmids used in this study

Name	Characteristics	Source
pVT100U	2µ ADH URA3	(Vernet et al., 1987)
pVT100U mtALP	2µ, ADH, URA3	This study
pVT100U cytALP	2µ, ADH, URA3	This study
pVT100U mtGFP	2µ, ADH, URA3	(Westermann and Neupert, 2000)
pYX242	2µ, TPI, LEU2	Novagen
pYX242 mtALP	2µ, TPI, LEU2	This study
pYX242 cytALP	2µ, TPI, LEU2	This study
Yep213	2µ, LEU2	(Otsuga et al., 1998)
Yep213 Dnm1a	2µ, LEU2	(Otsuga et al., 1998)
Yep213 Dnm1 K41A	2µ, LEU2	(Otsuga et al., 1998)
Yep213 Dnm1 S42N	2µ, LEU2	(Otsuga et al., 1998)
pHS12 mtDsRed.T3	CEN, ADH, LEU2	(Bevis and Glick, 2002)
pRS316	CEN, URA3	(Sikorski and Hieter, 1989)
pRS316 GFP-Atg8	CEN, URA3	This study
pRS313 GFP-Atg8	CEN, HIS3	This study
pRS323 mtDsRed.T4	2µ, TPI HIS3	(Jakobs et al., 2003)
pRS416 Fis1	CEN, URA3 515 bp 5′-UTR & 238 bp 3′-UTR from FIS1	This study
YPlac33 WHI2	CEN, URA3, 5′-UTR WHI2	(Cheng et al., 2008)
pVT100U WHI2-His	2µ ADH URA3	This study